2044

MASTER

ORNL-4712
UC-80 – Reactor Technology

# FINAL REPORT ON THE SECOND FUEL ROD FAILURE TRANSIENT TEST OF A ZIRCALOY-CLAD FUEL ROD CLUSTER IN TREAT

R. A. Lorenz
G. W. Parker

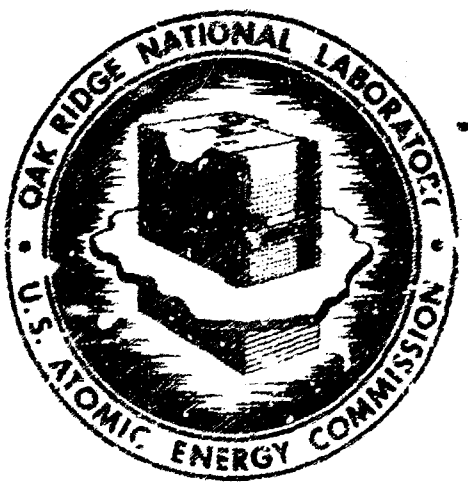


OAK RIDGE NATIONAL LABORATORY
operated by
UNION CARBIDE CORPORATION
for the
U.S. ATOMIC ENERGY COMMISSION

BLANK PAGE

Printed in the United States of America. Available from
National Technical Information Service
U.S. Department of Commerce
5285 Port Royal Road, Springfield, Virginia 22151
Price: Printed Copy $3.00; Microfiche $0.95

BLANK PAGE

ORNL-4710

Contract No. W-7405-eng-26

REACTOR CHEMISTRY DIVISION

# FINAL REPORT ON THE SECOND FUEL ROD FAILURE TRANSIENT TEST OF A ZIRCALOY-CLAD FUEL ROD CLUSTER IN TREAT

R. A. Lorenz C. W. Parker



JANUARY 1972

OAK RIDGE NATIONAL LABORATORY
Oak Ridge, Tennessee 37830
operated by
UNION CARBIDE CORPORATION
for the
U.S. ATOMIC ENERGY COMMISSION

CONTENTS

# FINAL REPORT OF THE SECOND FUEL ROD FAILURE TRANSIENT TEST OF A ZIRCALOY-CLAD FUEL ROD CLUSTER IN TREAT

R. A. Lorenz G. W. Parker


## ABSTRACT

The second fuel rod failure experiment in the Transient Reactor Test Facility (TREAT) was performed with a seven-rod bundle of 27-in.-long, Zircaloy-clad $UO_2$ fuel rods in a flowing steam atmosphere. A water-reactor loss-of-coolant accident was simulated by operating the TREAT reactor at constant power for 30 sec so that fission heat in the $UO_2$ pellets caused the Zircaloy cladding temperature to rise 80°F/sec to a maximum of approximately 2400°F. The fuel rods were initially pressurized with helium to between 65 and 75 psia (77°F) to simulate accumulated fission gas.

The Zircaloy cladding swelled and ruptured. The amount and distribution of swelling could result in the blockage of 91% of the bundle coolant channel area of a Boiling Water Reactor (BWR) at the location of maximum swelling. The average rod maximum circumferential swelling was 60%. Metallographic examination revealed ductile ruptures and significant oxygen pickup. Zirconium-steam reaction was 1.1%.

The center rod was preirradiated to 2800 MWd/MT in the Materials Testing Reactor (MTR) and Engineering Test Reactor (ETR) to build up an inventory of fission products and to determine irradiation effects on fuel rod failure characteristics. No irradiation effect was seen on the swelling and rupture characteristics from this low-level irradiation.

The release of gaseous fission-product $^{85}Kr$ from the irradiated center rod was approximately 0.5%. The release of volatile fission products $^{129}I$, $^{131}I$, and $^{137}Cs$ was slightly lower. Approximately 2.5% of the $^{131}I$ released from the center rod was in a chemically unreactive form, probably $CH_3I$.


---

## INTRODUCTION

With modern light-water power reactors, one of the most serious postulated accidents is the loss-of-coolant accident (LOCA) in which coolant water is lost through a break in the primary piping system. Emergency core-cooling systems (ECCS) have been designed and installed

# BLANK PAGE

in these reactors to provide emergency cooling in the unlikely occurrence of such a postulated accident.[1] Zircaloy cladding of the fuel rods would undergo a severe temperature transient during a LOCA as a result of redistribution of heat stored in the $UO_2$ fuel during the short time interval between blowdown of the cooling water and complete application of the emergency cooling water. Many of the fuel rods would bow, swell, and rupture before the emergency cooling performed its function. Continued heating of the Zircaloy cladding from fission-product decay heat and from the reaction of Zircaloy with steam at high temperature would result in embrittlement of the cladding and gross damage to the core accompanied by the release of large amounts of fission products if the emergency coolant could not adequately cool the core.

A fuel rod failure study program was initiated at Oak Ridge National Laboratory in July 1968 as part of the ORNL Nuclear Safety Program[2,3,4,5] in order to determine the characteristics and extent of fuel rod failure on emergency cooling effectiveness. The program at ORNL includes transient (rapid heating) burst tests of single and clustered Zircaloy tubes in inert atmosphere, heat transfer and cladding behavior during the blowdown phase of the LOCA, high temperature rupture tests of irradiated fuel rods in steam atmosphere, and rupture tests of clusters of fuel rods in steam atmosphere in the Transient Reactor Test Facility (TREAT) reactor. A summary report describing the effects of fuel rod failure was published in Nuclear Safety.[6]

The final report of the first fuel rod failure experiment performed in TREAT (FRF-1) was published[7] earlier and this reports covers the second experiment in TREAT (FRF-2). Each experiment used a test assembly consisting of a seven-rod cluster of 27-in.-long, Zircaloy-clad $UO_2$ fuel rods exposed to a flowing steam atmosphere in simulation of steam flow conditions immediately following the blowdown portion of the LOCA. The center rod contained fission products from a preliminary irradiation to a fuel burnup of 650 MWd/MT (FRF-1) or 2800 MWd/MT (FRF-2) to test the effect of irradiation on rupture characteristics as well as to provide a fission-product inventory for fission-product release measurements. The rods were prepressurized with helium which simulated fission gas pressure accumulated after high burnup. The fuel rod failure tests were

performed in TREAT by operating the reactor at steady power so that fission heat in the $UO_2$ pellets raised the cladding temperature in duplication of LOCA temperature behavior immediately following coolant blowdown. Maximum cladding temperatures were approximately 1800°F in FRF-1 and 2400°F in FRF-2.

Because fissioning in the $UO_2$ pellets was used as the heat source in these experiments, the heat transfer conditions between pellet and cladding were much as would be expected in the LOCA. The TREAT fuel rod failure experiments are therefore considered to be proof-tests of the data and behavioral models derived in the other tube-burst and fuel rod rupture research tasks.

## DESCRIPTION OF EQUIPMENT - TREAT FUEL ROD FAILURE EXPERIMENT FRF-2

### General Description

A photograph of the in-reactor components of the equipment is shown in Fig. 1. Fuel rod cladding was of a nominal 0.564-in. diameter and the rods were located on an equilateral triangle spacing 0.75 in. apart. The rods occupied 51% of the cross-sectional area in the triangular lattice and 37% of the area within the 2.45-in.-I.D., 0.010-in.-thick, gold-plated stainless steel sleeve surrounding the rod bundle. Steam flowed up through the rod bundle at a rate of 10 ℓ/min (STP) along with 1.8 ℓ/min (STP) helium at a pressure of about 19 psia. The steam-helium mixture carried fission products from the ruptured rods through a filter pack where the aerosol particles and most of the iodine were collected. The entire steam system was preheated electrically to 265°F to prevent condensation of steam. The primary vessel was well insulated to prevent overheating of the reactor fuel when the fuel rods of the experiment underwent the LOCA temperature transient.

The flow system is shown in Fig. 2. Heat in-put to the steam generator provided 8-g/min steam flow to the bottom of the rod bundle. Helium flowing at 1.8 liters/min (STP) was mixed with the steam in the generator, and the mixture was passed through a filter pack after leaving the primary vessel. Based on the available surface area of Zircaloy in the fuel element, these flow rates correspond to 29,500/lb/hr steam flow

PHOTO 93731AR

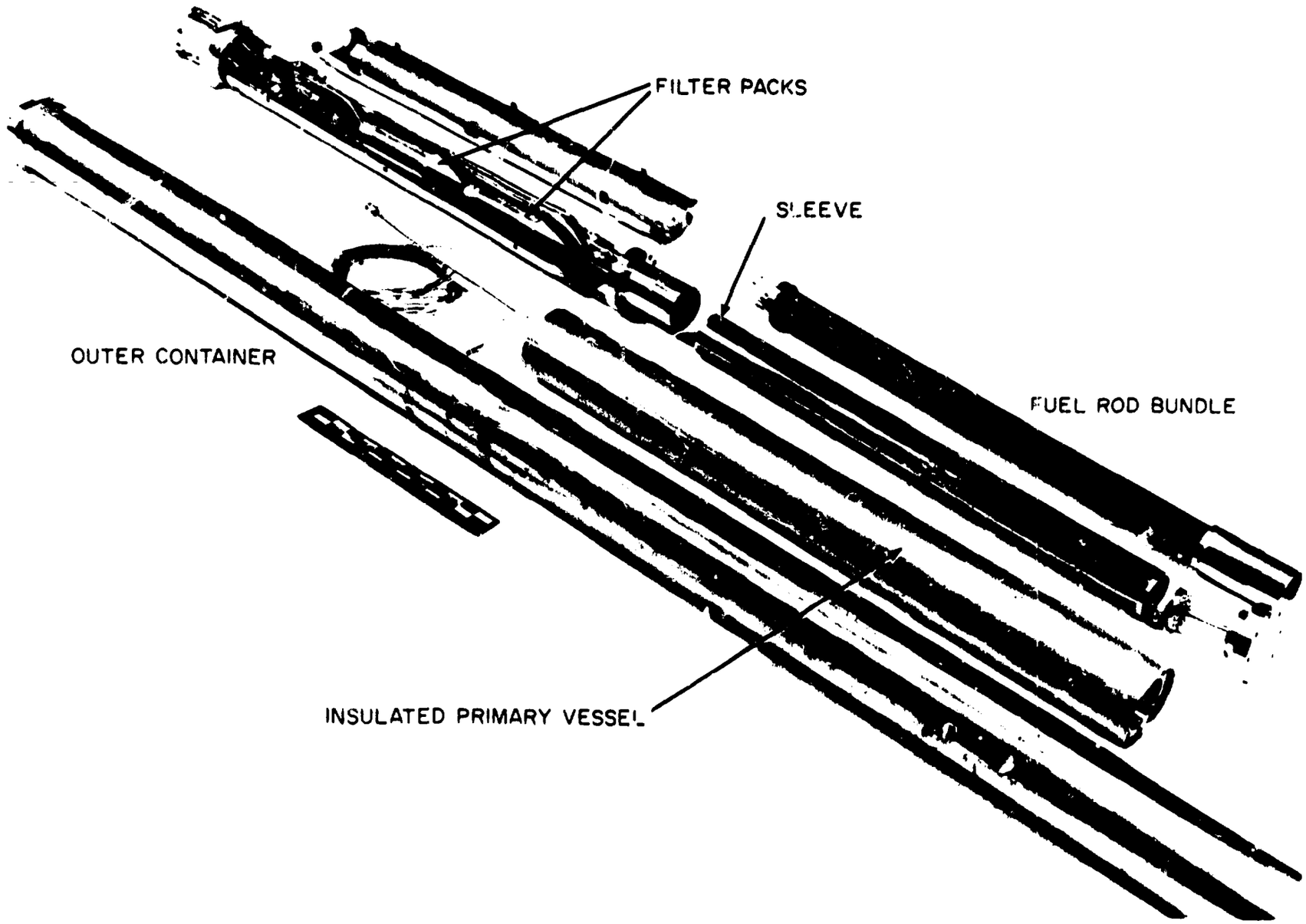


Fig. 1. In-Reactor Components of the Equipment for FRF-2.

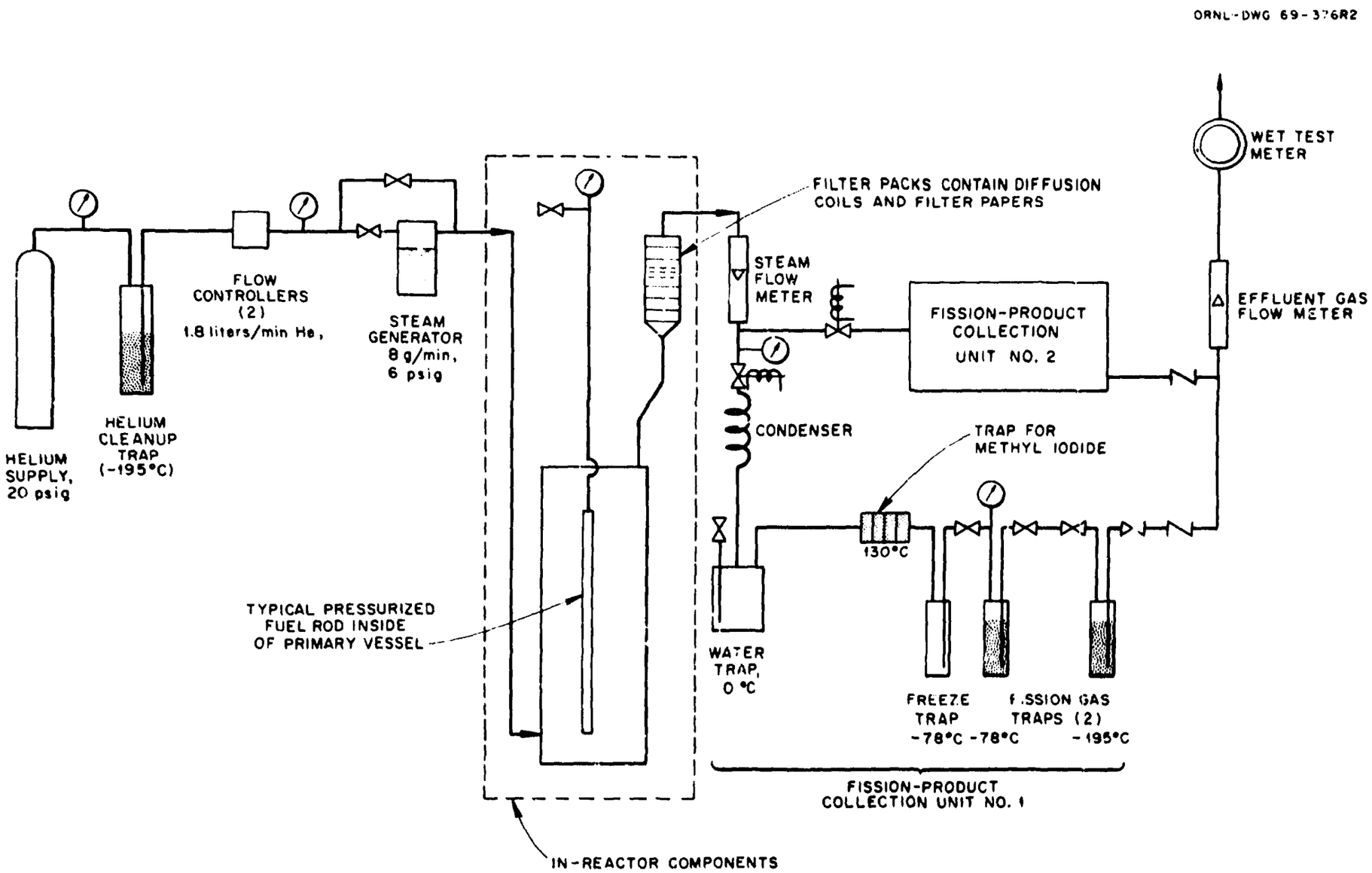


Fig. 2. Schematic Flow Diagram of Equipment for TREAT Fuel Rod Failure Experiment FRF-2.

at 70 sec after blowdown for a 2,250 MW(t) BWR and 24,200-lb/hr steam flow at 12 sec after shutdown for a 2,760 MW(t) PWR. These values are published estimates of residual water boiloff following the blowdown.[8] In the filter pack, chemically reactive iodine compounds deposited on silver-plated surfaces, and aerosol particles were collected on three fiberglass-asbestos filters in series. The steam was condensed outside the reactor, and helium carried the remaining volatile fission products through a warm iodine-impregnated charcoal trap for collection of $CH_3I$ and through liquid-nitrogen-cooled charcoal traps for collection of xenon and krypton. Effluent helium was monitored by a rotameter and a wet-test meter. Hydrogen formed by the reaction of steam with zirconium appeared as effluent gas flow greater than the controlled helium flow. Only one filter pack was used in FRF-2, but a second identical external fission-product gas collection system was used after the first 90 seconds in order to measure slowly released volatile fission products.

## Fuel Rod Construction and Suspension

Details of fuel rod construction are given in Table 1. The fuel rods were assembled at ORNL with Zircaloy-4 cladding of recent commercial manufacture and selected fuel pellets from surplus Dresden-I fuel rods. All cladding was inspected ultrasonically for flaws by using a standard defect groove 0.001 in. deep and 1/8 in. long. No defects were found. Wall thickness variations were also determined ultrasonically. Rods 11, 12, and 13 were cut from one length of tubing and had more uniform wall thickness than rods 16, 17, and 18 which were cut from another length of tubing. The fuel rod plenums contained springs wound from 1/16-in.-diameter Zircaloy wire, but the rods were assembled without compression on the springs. A 3/8-in.-long Zircaloy cylinder with a 1/16-in. by 1/16-in. groove for free gas passage was located between the spring and first pellet.

A 1/8-in.-diam Zircaloy tube with a 1/16-in.-diam hole was welded to the top of each rod for pressurizing. The rods were held at 255°F and evacuated overnight for drying and outgassing. The void volume was measured by expanding helium into the rod from a known volume. Pressure was increased to the desired level and the tube was pinched from the

Table 1. Characteristics of Fuel Rods Used in Experiment FRF-2

| | Center Rod 58-3 | Rod 11 | Rod 16 | Rod 12 | Rod 17 | Rod 13 | Rod 18 |
|---|---|---|---|---|---|---|---|
| Cladding outside diameter, in. | 0.5638 | 0.5633 | 0.5633 | 0.5633 | 0.5632 | 0.5633 | 0.5632 |
| Cladding inside diameter, in. | 0.4987 | 0.4999 | 0.4996 | 0.4993 | 0.4994 | 0.5001 | 0.4992 |
| Cladding wall thickness, in. | | | | | | | |
| Minimum | 0.0326 | 0.0305 | 0.0291 | 0.0311 | 0.0292 | 0.0307 | 0.0296 |
| Maximum | | 0.0328 | 0.0345 | 0.0328 | 0.0345 | 0.0324 | 0.0344 |
| Pellet diameter, in. | | | | | | | |
| Minimum | 0.487 | 0.493 | 0.493 | 0.493 | 0.492 | 0.493 | 0.492 |
| Maximum | 0.493 | 0.495 | 0.495 | 0.496 | 0.4945 | 0.495 | 0.494 |
| $UO_2$ weight (1.51% enriched), g | 736 | 743 | 739 | 743 | 736 | 740 | 740 |
| Normal $UO_2$ weight, g | 30 | 29 | 29 | 29 | 30 | 25 | 28 |
| Pelnum length, in. | 2-1/2 | 2-5/16 | 2-9/16 | 2-3/8 | 2-5/16 | 2-3/8 | 2-7/16 |
| Plenum volume, $cm^3$ | 7.2 | 6.7 | 7.4 | 6.8 | 6.7 | 6.8 | 7.0 |
| Cladding gap and pellet gap voids, $cm^3$ | 3.9 | 4.7 | 4.5 | 5.2 | 5.2 | 5.3 | 5.0 |
| Pressure cell and tubing voids, $cm^3$ | 0 | 2.2 | 0 | 2.2 | 0 | 0 | 0 |
| Total gas space, $cm^3$ | 11.1 | 13.6 | 11.9 | 14.2 | 11.9 | 12.1 | 12.0 |
| Pressure, psia He at 77°F | 65 | 75 | 75 | 75 | 75 | 75 | 75 |
| Helium in rod, $cm^3$ (STP) | 45 | 64 | 56 | 66 | 56 | 57 | 56 |

outside onto a 1/16-in.-diam gold wire located in the tube. The pinch seal was checked for leakage, and the tube was then cut and seal welded. A final leak check was made with a mass spectrometer helium leak detector. After assembly, the Zircaloy-4-clad rods were autoclaved for two days in 1500-psi steam at 750°F. The helium fill pressure range of 65 to 75 psia (77°F) was based on estimates of fission-gas pressure in a BWR calculated by the D′ (empirical) method.[9] The calculation showed that this pressure range is typical for a mature core of a BWR but that almost all the volatile fission products released from $UO_2$ into the rod void spaces would originate in rods with pressure above this range.

Rods 11 and 12 were connected to strain-gage pressure transducers for continuous monitoring of internal pressure. Platinum vs Pt-10% Rh thermocouples made of 30-gage wire (0.010 in. diam) were spot-welded directly to the cladding of rods 11, 12, and 13 to monitor cladding temperature. The thermocouple wires were insulated with $Al_2O_3$ and supported on the rods with single loops of 0.010-in.-diam Pt-10% Rh wire.

The outer six rods were suspended from the top support by U-shaped clips that allowed bowing but prevented rotation. The irradiated center rod was inserted remotely from the bottom of the primary vessel in the TAN (Test Area North) hot cell at NRTS (National Reactor Testing Station) as the last operation before moving the completed assembly to TREAT. The cap of the center rod contained splines and a detent groove for engagement with spring-loaded balls on the upper support spider so that it hung freely but could not rotate. The center rod had 5/16 in. available for linear expansion and the outer rods had 15/16 in.

## Center Rod Irradiation

The center rod was irradiated as experiment ORNL-58-3 for a short cycle (No. 295) in the MTR in June 1969 and for a long cycle (No. 104) in the ETR in October and November 1969. Based on a postexperiment burnup analysis, the peak linear power was 13.9 kW/ft, considerably lower than the desired 18 kW/ft. Peak burnup was 2800 MWd/MT. Magnesium alloy spacers in the irradiation assembly provided insulation between the Zircaloy-4 cladding and the relatively cool reactor cooling water, so the cladding temperature was close to that found in power reactors.

After the irradiation in the ETR, the rod was neutron radiographed and gamma scanned with a lithium-drifted germanium detector and a 0.005-in. slit-width collimator. The neutron radiograph showed that there were no central voids in the $UO_2$ pellets. An axial void would be expected from grain growth and sintering at $UO_2$ center-line temperatures above 3400°F. The gamma scan showed uniform fission-product concentrations at pellet centers and at pellet interfaces, a further indication that the $UO_2$ temperature during irradiation was lower than the design temperature. After the gamma scan and the neutron radiograph had been made the rod was removed from its irradiation capsule and installed in the center of the TREAT experiment bundle in the TAN hot cells.

## EXPERIMENTAL PROCEDURE

The fuel rod failure experiment was performed in TREAT on March 11, 1970. A calibration transient was performed at low reactor energy output to confirm the calculated rise in cladding temperature for a given reactor energy release. The loss-of-coolant transient then proceeded according to the following schedule:

| Time | Operation |
|---|---|
| -2 hr | Steam system electrically preheated; helium flow 1.8 liters/min (STP) |
| -8 min | Steam flow started, 10 liters/min |
| 0 min | TREAT transient started |
| 6 sec | Reactor power reached 30 MW, power held between 20 and 40 MW |
| 30.3 sec | Cladding temperature 2190°F; first rod ruptured |
| 30.8 sec | Cladding temperature 2220°F; rod 11 ruptured |
| 31.0 sec | Third rod ruptured |
| 32.9 sec | Cladding temperature 2300°F; rod 12 ruptured |
| 33.8 sec | Fifth rod ruptured |
| 34.7 sec | Sixth rod ruptured |
| 35.0 sec | Reactor scrammed |
| 37.5 sec | Cladding temperature 2400°F; seventh rod ruptured |
| 90 sec | Flow changed to fission-product gas collection unit No. 2 |

| Time | Operation |
|---|---|
| 15 min | Heat to steam generator turned off |
| 17.5 min | Flow changed back to gas collection unit No. 1 |
| 20 min | Steam generator bypassed |
| 31 min | Flow stopped. |

## EXPERIMENTAL RESULTS

### Pressure, Temperature, and Flow Rates

A variety of temperature, pressure, flow rate, and power data was obtained during the loss-of-coolant test in TRF T. Measured power, cladding temperature, and rod internal pressures are shown in Fig. 3. The cladding temperature rate of rise averaged 80°F/sec. Temperatures measured in the primary vessel, filter pack, etc. are given in Table 2. Higher temperatures were reached in this experiment because of the 724-MWsec transient compared with 556 MWsec in experiment FRF-1 and also because of a gold-plated, heat-reflective sleeve around the bundle reduced heat loss. Temperature gradients can be estimated from data in Table 2.

Rods 11 and 12 were connected to pressure transducers for continuous pressure measurement. The peaking of the pressure curves at 23 sec (1620°F) corresponded to the beginning of significant volume increase. The Zircaloy phase change showed as a thermal arrest at this temperature.

System pressure and flow rate are shown in Fig. 4. Steam flow was determined by measuring the temperature increase in cooling water required to condense the steam. An uncompensated time-response delay of about 5 sec was caused by the volume of the filter pack and tubing leading to the steam condenser. The increase in steam flow at 26 sec was probably a result of temperature increase around the rod bundle. The decrease in flow after 26 sec was probably a result of steam being consumed by the steam-zirconium reaction.

### Metal-Water Reaction

A wet-test meter at the outlet of the flow system measured combined helium and hydrogen flow. The volume of noncondensable gas (Fig. 4 was obtained by subtracting the constant helium inlet flow. Pressure and temperature changes in the system caused the helium carrier gas to fluctuate an

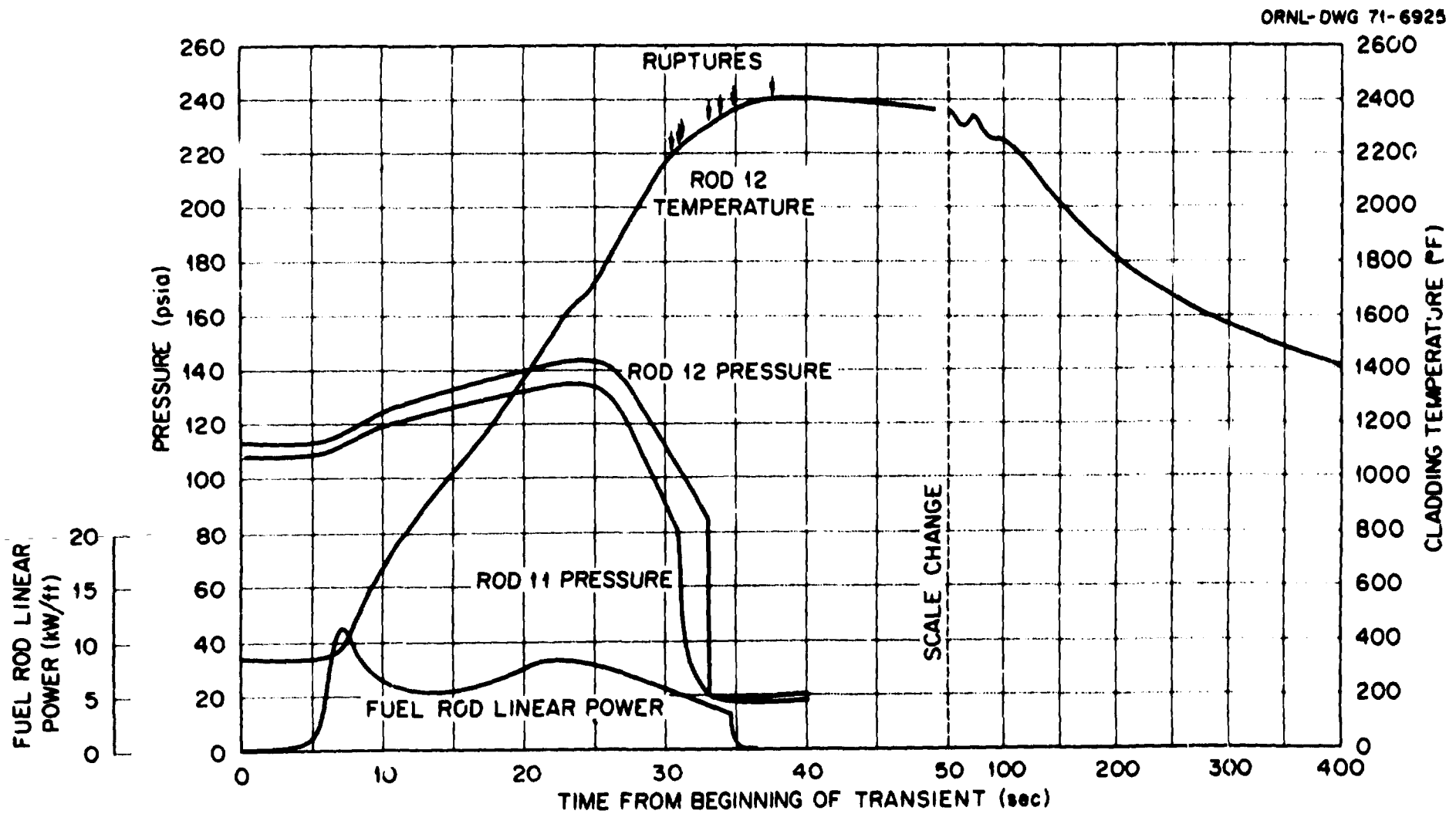


Fig. 3. Pressure and Temperature in TREAT Experiment FRF-2.

Table 2. Temperature Measurements in Experiment FRF-2

| Location (Rod-T.C. No.) | (12-4) | (13-4) | (12-2) | (12-1) | (13-2) | (13-1)[a] | Primary Vessel, Center | Filter Pack |
|---|---|---|---|---|---|---|---|---|
| Distance Below Top Shoulder (in.) | 10.7 | 13.9 | 14.8 | 14.8[b] | 18.9 | 18.9[b] | -- | -- |
| Time (sec) | | | | Temperature (°F) | | | | |
| 0 | 333 | 333 | 327 | 326 | 333 | 333 | 324 | 266 |
| 5 | 335 | 333 | 329 | 327 | 335 | 334 | | |
| 10 | 684 | (c) | 702 | 713 | 676 | 672 | | |
| 15 | 1031 | | 1054 | 1068 | 1029 | 1018 | 342 | 277 |
| 20 | 1375 | 1361 | 1411 | 1415 | 1379 | 1368 | | |
| 25 | 1733 | 1712 | 1805 | | 1738 | 1749 | | |
| 30 | 2177 | 2131 | | | 2221 | | 374 | 298 |
| 35 | 2368 | 2377 | 2325 | | | | | |
| 45 | 2384 | 2436 | 2358 | | | | 392 | 309 |
| 60 | 2302 | 2399 | 2349 | | | | 417 | 307 |
| 180 | 1868 | | | | | | 741 | 298 |
| 20 min | | | | | | | 885 | 291 |
| 30 min | | | | | | | 806 | 243 |

[a] Because of suspected amplifier zero shift, the output of this thermocouple was increased by 0.160 mv (36°F at lowest temperature and 25°F at highest temperature).

[b] These thermocouples were located on cladding facing the outside of the bundle. All other couples were located toward the inside of the bundle.

[c] Blank spaces for rod temperatures indicate open thermocouples.

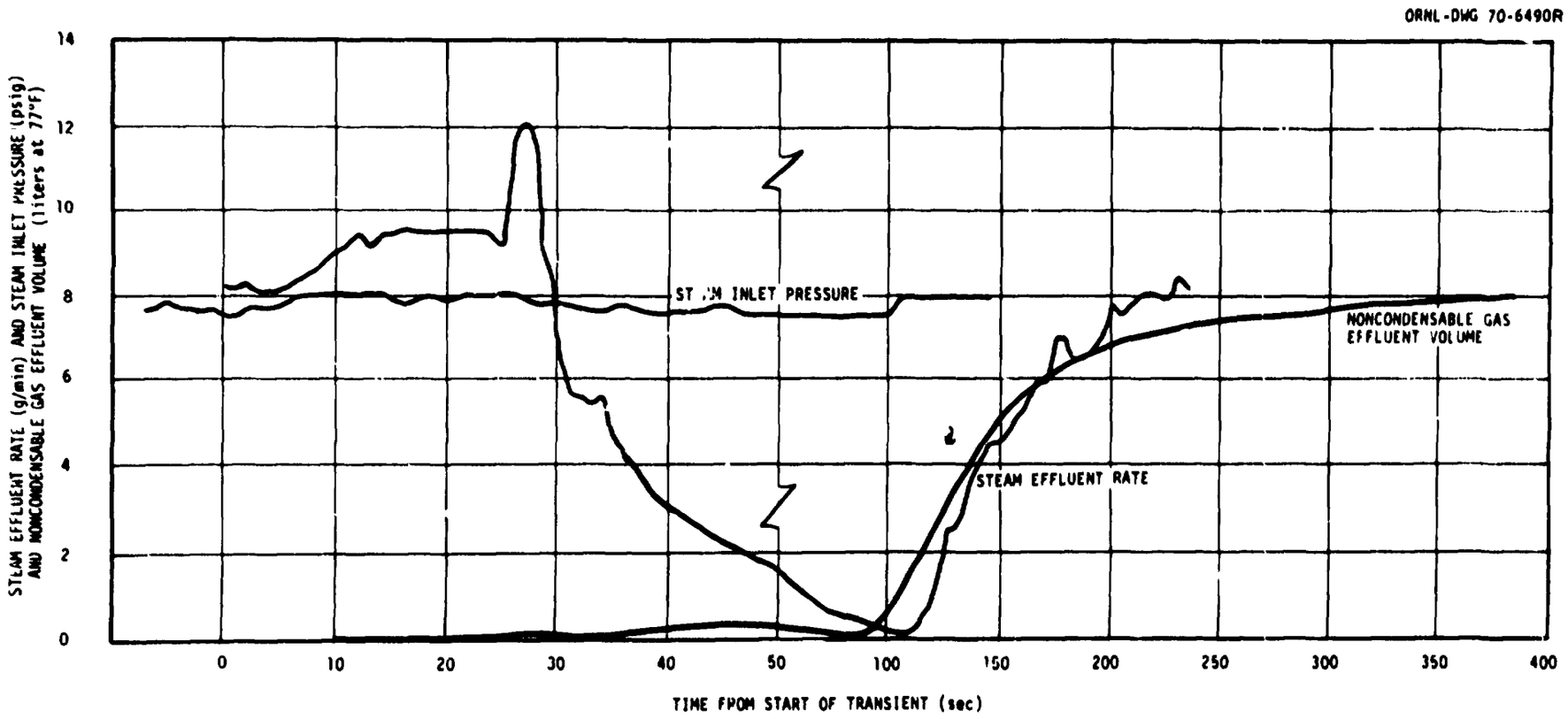


Fig. 4. System Flow During TREAT Experiment FRF-2.

unknown amount at the wet-test meter location, but the fluctuations averaged out over a several-minute period when pressure returned to normal. Approximately 130 sec is required for gas to flow from the primary vessel to the wet-test meter, but an increased indication of flow should begin much sooner, depending on flow restriction in the system. Allowing for 400 $cm^3$ of helium released from the rods and for temperature changes in the system, the hydrogen formed by steam-zirconium reaction was calculated to be 5.5 ± 1 liters (STP). This is equivalent to about 1.1% metal-water reaction based on the amount of cladding on the seven rods. Calculations for metal-water reaction during loss-of-coolant accidents in power reactors have indicated less than 1% reaction.[10]

## Examination of the Fuel Rod Bundle

The experimental assembly was returned to ORNL for disassembly and examination. The filter pack was removed for radiochemical analysis, and the fuel rod bundle was removed and photographed. Figure 5 is a photograph of the bundle after removal from the primary vessel. A heavy white oxide layer was apparent mainly at the bottom of the bundle and on the outer surfaces of the rods. The original shiny black oxide remained at the top around the rod plenums. The bowed center rod is visible between rods 18 (left) and 13 (right). Figure 6, a view of the other side of the bundle, shows the swollen portions of rods 12 (left) and 16 (right).

Figure 7, a drawing of the fuel bundle arrangement, shows the direction of rupture. The approximate amount of swelling at 16-3/4 in. below the fuel rod top shoulders, near the bottom of the rupture zone, is indicated by dashed circles. Swelling was not exactly circular, however, and the rods actually bowed outward to accommodate the "overlapping." The swollen rods at the 16-3/4-in. level occupy a 4.0-$in.^2$, cross-sectional area compared with the 3.81 $in.^2$ available for seven rods and their associated flow channels in a modern BWR. The BWR rods occupy 46% of this available area, in contrast with 51% for the rods in the equilateral triangular lattice of TREAT and 37% inside the heat-reflective sleeve. The relatively large heat-reflective sleeve was used to help minimize radial temperature differences.


Fig. 5. Bundle of Zircaloy-Clad Fuel Rods from Experiment FRF-2 Showing White Oxide Toward Bottom (Steam Inlet) and Original Black Oxide Around Plenums at Top.

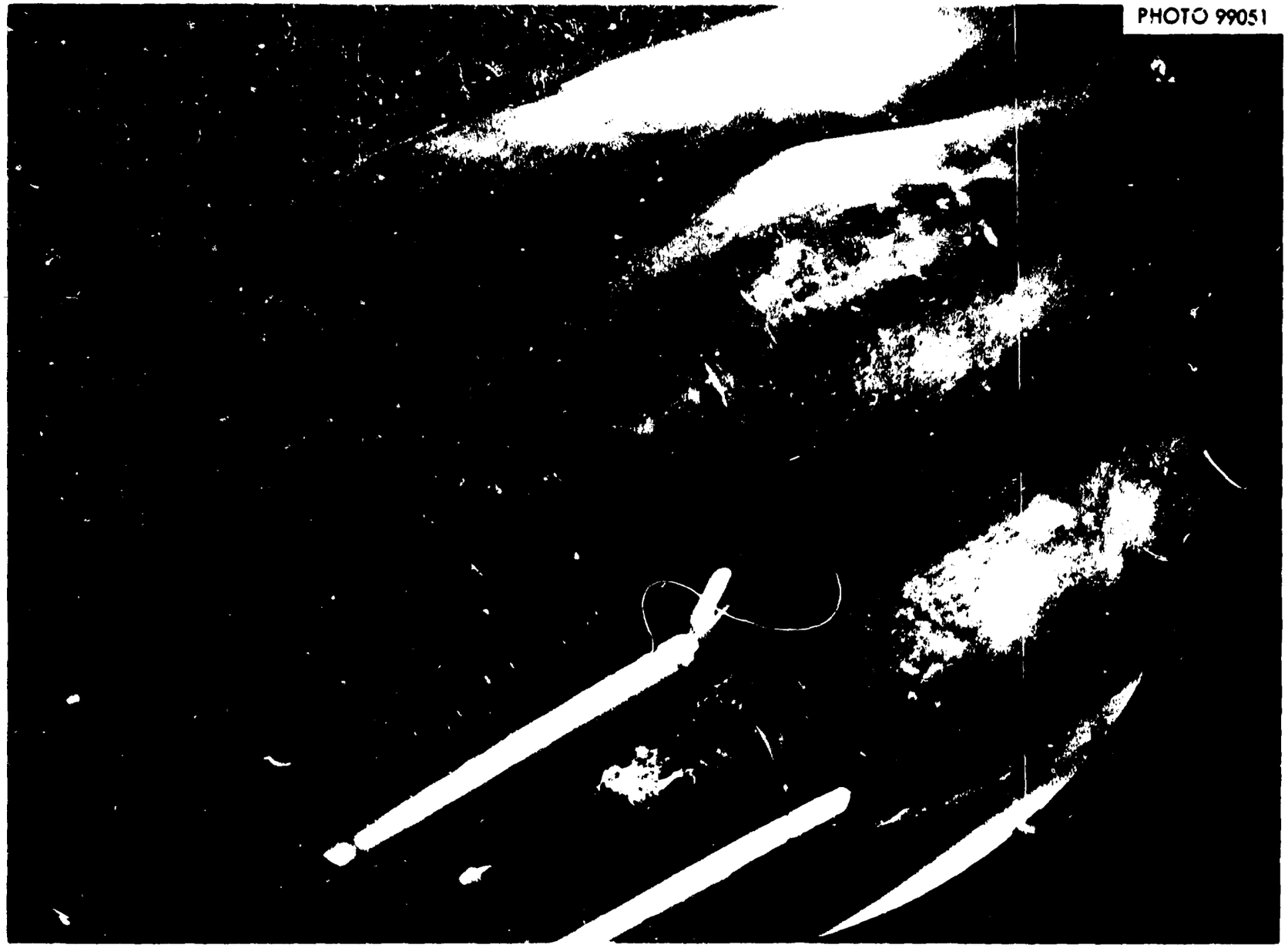


Fig. 6. Closeup View of Swollen Areas on Rods 12(Left) and 16 (Right) in Place in Bundle from Experiment FRF-2.

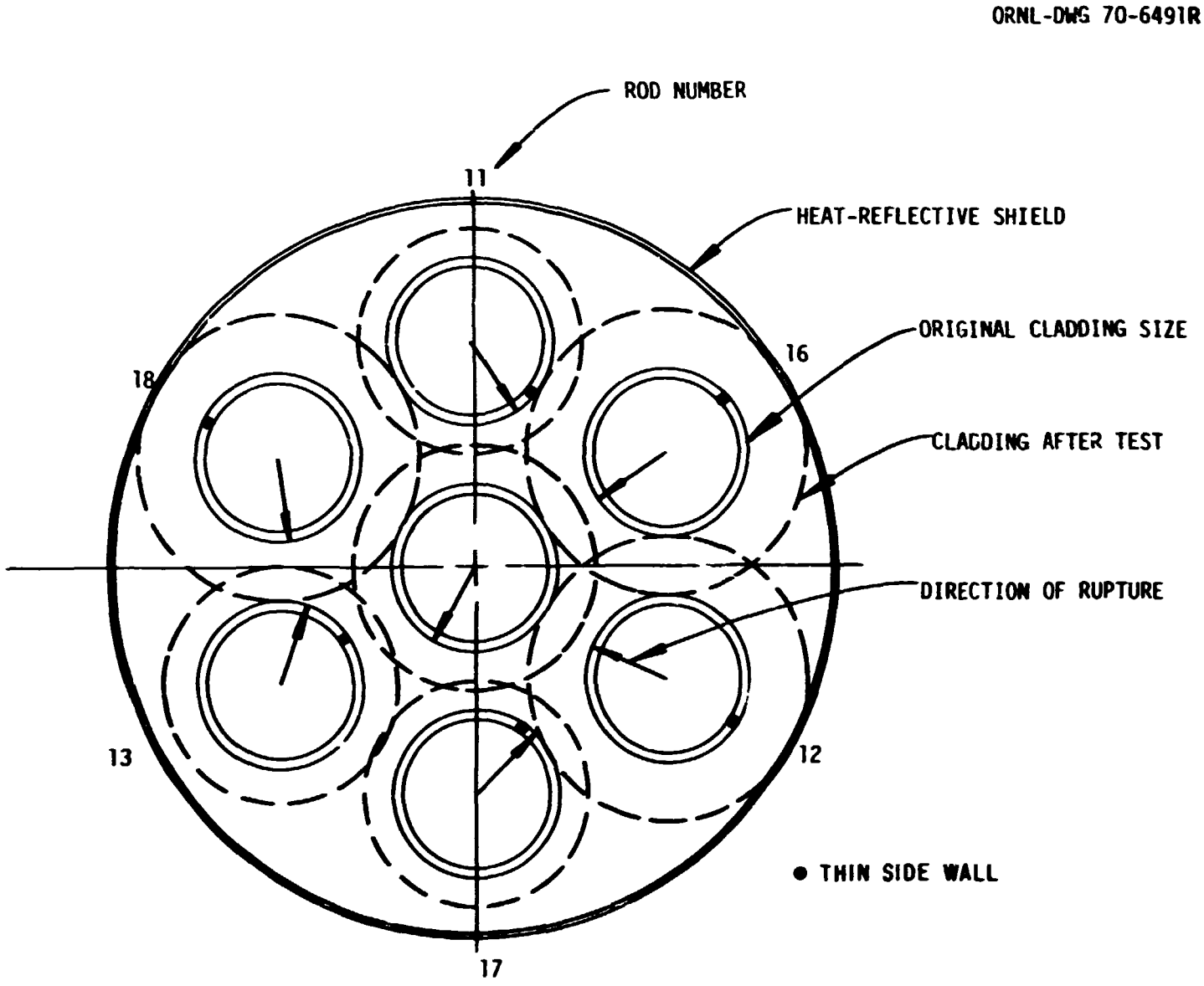


Fig. 7. Arrangement of Fuel Rods and Location of Ruptures in TREAT Fuel Rod Failure Experiment FRF-2.

Several of the rods showed stretch-marks where the differences in oxidation brought out vertical (axial) lines. Figure 8 illustrates this on rod 18 (center) and rod 13 (right) photographed from outside of the intact bundle. A temporary bottom spacer was used to keep the rods in their original spatial relationship during bundle photography. Figure 9 shows the bundle after two rods were removed. Surfaces in the interior of the bundle were generally coated with black oxide. The Pt-10% Rh wires used for supporting the thermocouples were strong enough to restrict swelling, as on rod 13 shown on the extreme right of Fig. 9. Closeup views of the center rod rupture and the wire constriction on rod 12 are given in Fig. 10. A eutectic formed between the wire and the Zircaloy. Eutectic formation between Inconel support clips and Zircaloy has been studied by several groups, who have concluded that there would be no detrimental effect either under normal or accident conditions.

## Fuel Rod Failure Characteristics

Figure 11 is a montage showing the rupture opening of the center rod and the other six rods located at their correct relative heights and perspective to the center rod. From left to right, the outer rods are in their correct orientation, clockwise when viewed from the top. The background paper contains 1/8-in. squares, and it may be seen that all the ruptures occurred within a 2-1/4-in. length. Views of the rods at 90° to the rupture are shown in Fig. 12.

Photographs of the center rod and direct measurements on the outer rods were used to measure swelling and increases in rod length. Table 3 shows that mean swelling at the largest bulge of the outer rods was about 60%. Increases in length averaged about 0.27 in. for the outer rods, or slightly more than 1% of the heated length. The center rod had only 0.31 in. available for linear expansion, neglecting expansion of the primary vessel, and it apparently contacted the bottom support. This caused sagging and the resultant corkscrew shape. The outer rods had more space for linear expansion and therefore did not receive support at the bottom. They remained relatively straight, except for being bowed outward enough to accommodate the swelling in the rupture region. The peak measured internal pressure in each rod resulted in an axial


Fig. 8. Rods 18 (Center) and 13 (Right) Coated with Heavy White Zirconium Oxide Formed by Rapid Reaction with Steam.

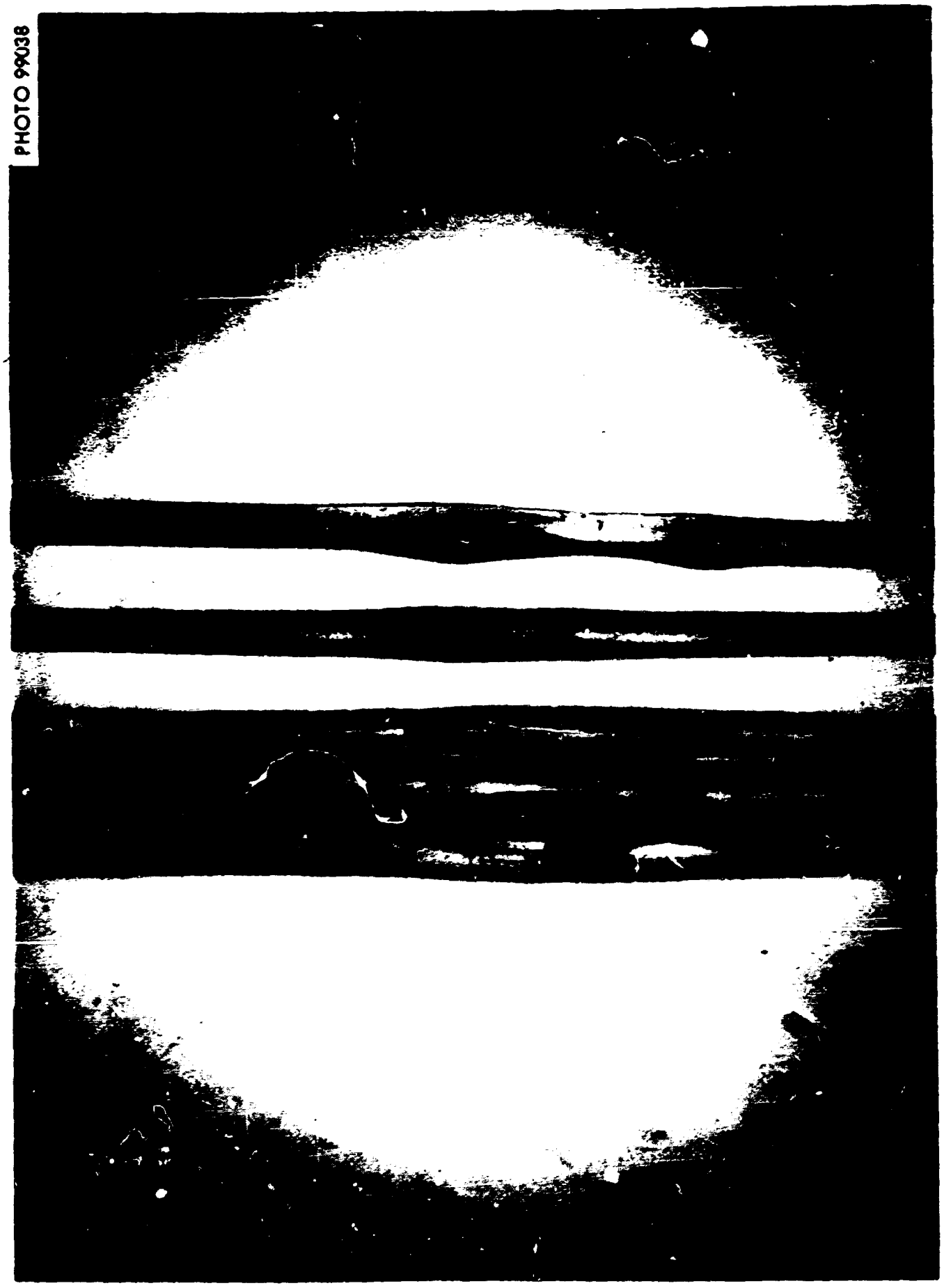


Fig. 9. Rods 17 and 13 (Far Right) Removed to Show Interior of Bundle (rods 16, Center, and 12).

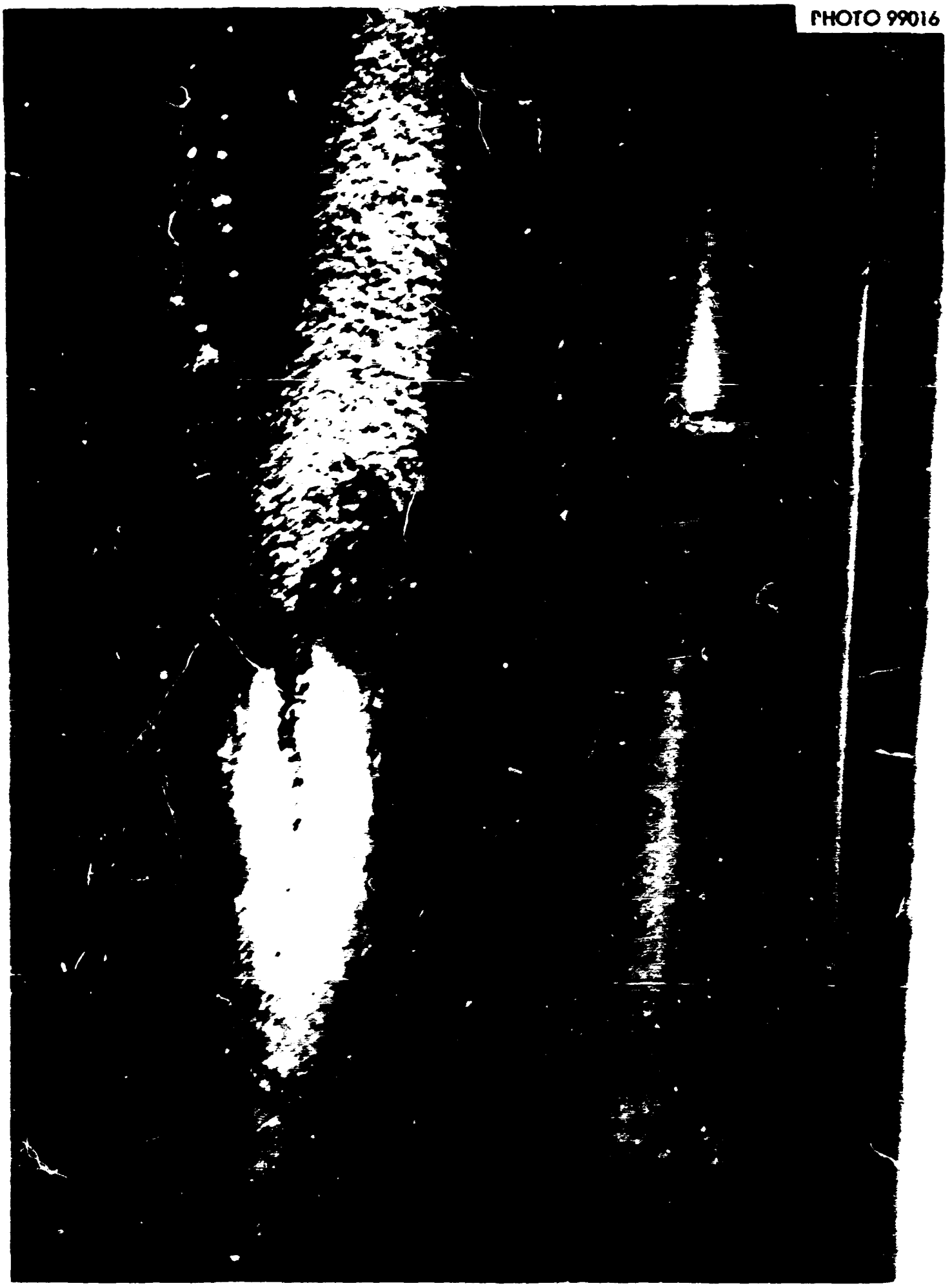


Fig. 10. Closeup View of Rupture in Center Rod and Pt-10% Rh Wire that Reacted with Zircaloy Cladding on Rod 12.

PHOTO 99254R

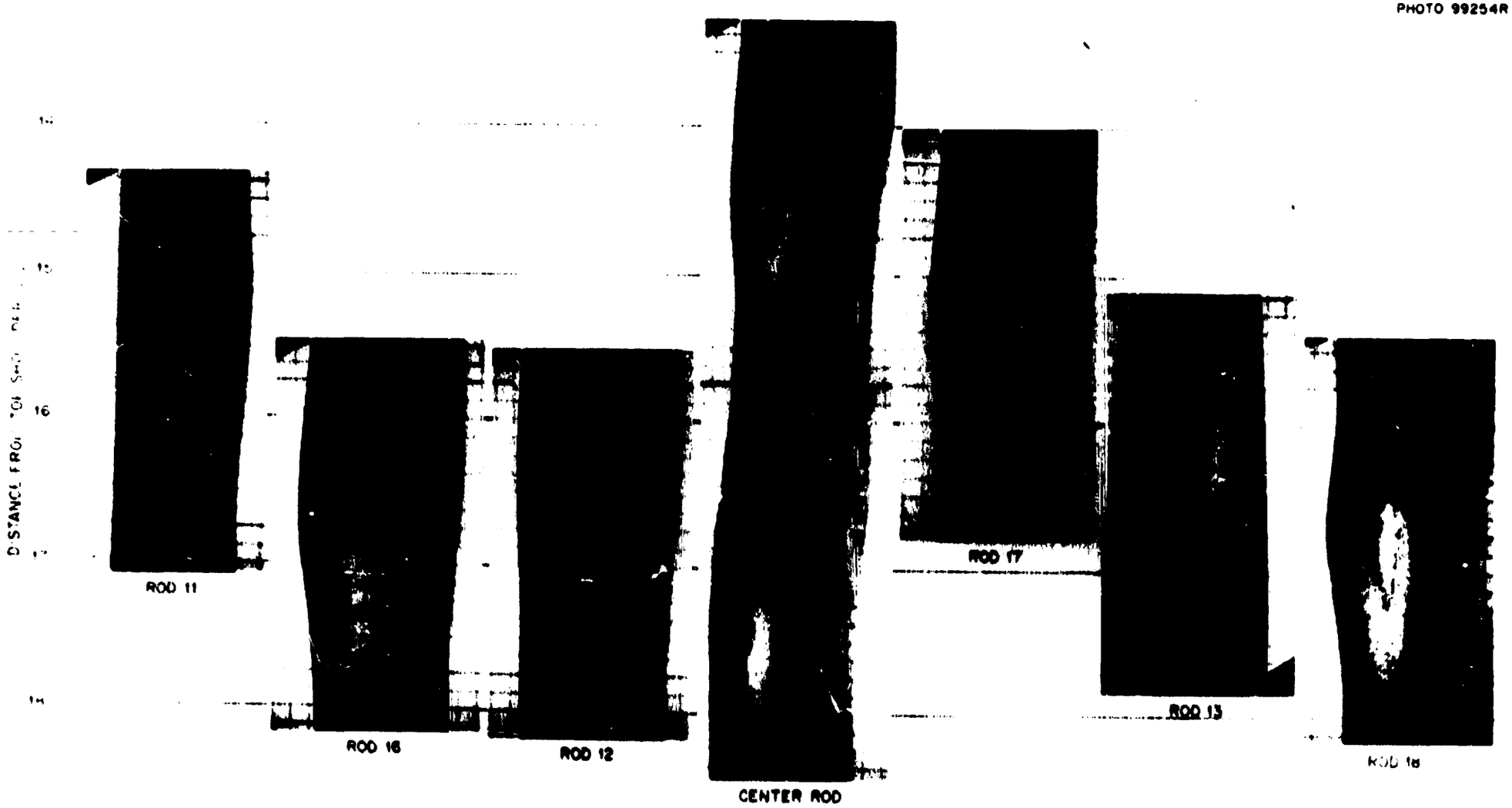


Fig. 11. Closeup Views of Ruptured Areas of Rods Used in Experiment FRF-2.

PHOTO 99255

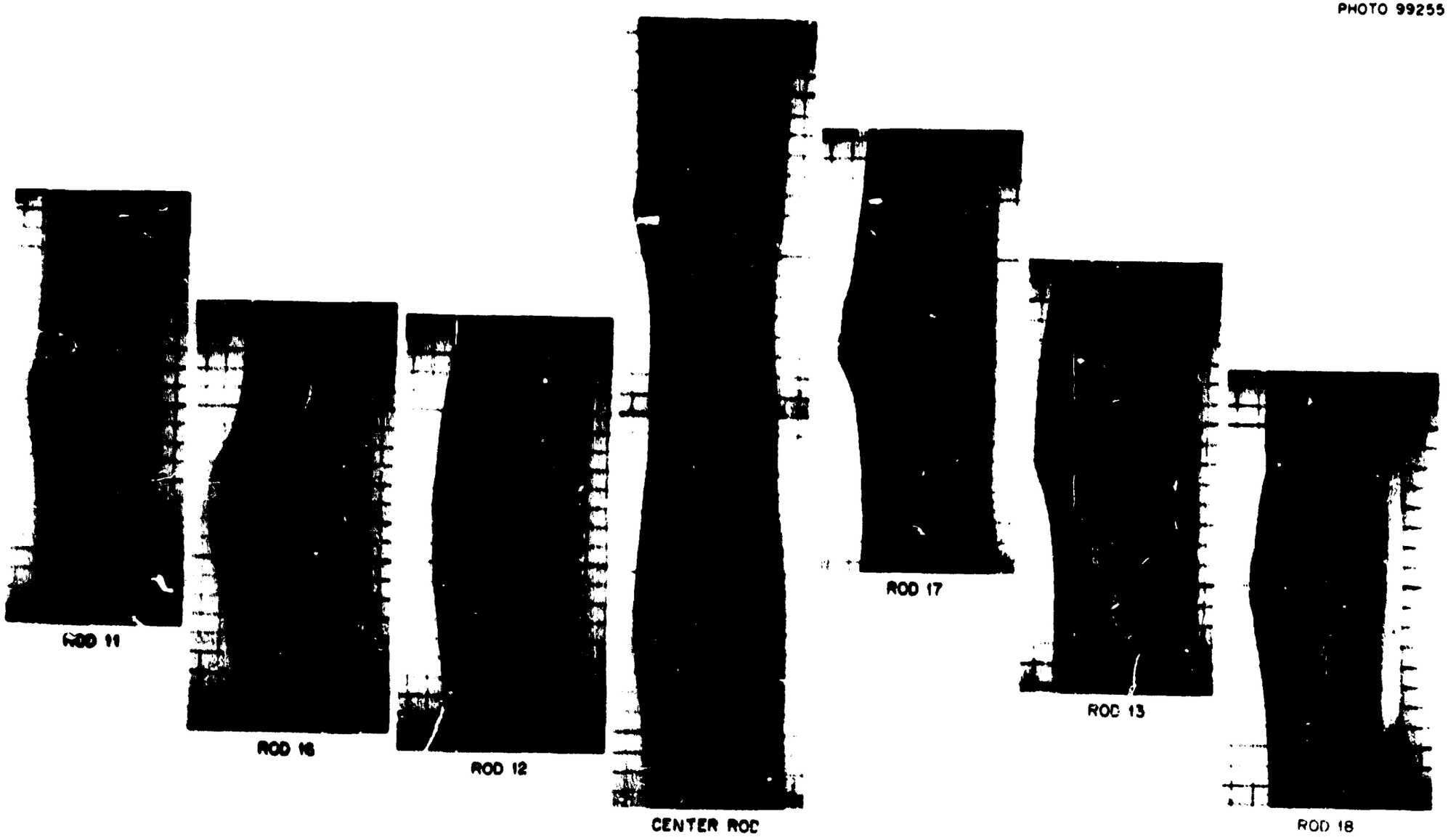


Fig. 12. Views of Ruptured Areas at 90° from Ruptures, TREAT Experiment FRF-2.

Table 3. Fuel Rod Dimensional Changes, Experiment FRF-2

| Rod Identification | Diam Increase, Rupture-to-Rack (%) | Diam Increase, Viewed by Center Rod (%) | Increase in Rod Length (in.) | Volume Increase From Swelling ($cm^3$) |
|---|---|---|---|---|
| Center (58-3) | 51 | 57 | 0.09 | 42 |
| 11 | 50 | 48 | 0.32 | 29 |
| 12 | 62 | 74 | 0.34 | 33 |
| 13 | 52 | 55 | 0.28 | 33 |
| 16 | 77 | 75 | 0.37 | 40 |
| 17 | 57 | 53 | 0.32 | 29 |
| 18 | 63 | 63 | 0.28 | 35 |

force of 25 lb, much greater than its weight - approximately 2 lb. Since reactor fuel rods are supported at the bottom and with spacers every 18 in. or so, it is believed that the form assumed by the center rod is typical of that to be expected in a reactor bundle.

### Metallographic Examination and Embrittlement Determination

Tubing cross-sections taken near the positions of maximum expansion for each of the six outer rods from TREAT experiment FRF-2 were mounted and polished for metallographic examination and microhardness measurements. Some oxide buildup was found on the outer surface of each tube. These buildups varied around the circumference of each section, apparently due to rechanneling of steam in the blocked section of the bundle. Oxide was also found on the inner surface of the tubes, but not to the extent observed on the outer surfaces. Oxygen penetration produced oxygen-stabilized $\alpha$ layers under the oxide.

Hardness measurements were taken at selected points on the cross section as shown in Fig. 13. The results of these are shown in Table 4. Tubes 11 and 18 had large sections of the wall broken away, but measurements were taken with the pattern shown in Fig. 13 and terminated at the break. The sharp edges of the rupture openings were missing from all tubes since the tubes were broken at the center before being potted. The nil-ductility temperatures shown in Table 4 were determined by Hobson from hardness measurements taken at mid-wall positions. Hobson used his previously determined correlation between hardness and nil-ductility temperature.[11,12] The temperatures are approximate because the nil-ductility curve was based on a full-wall-thickness tube; the tubes examined here were thinned by circumferential expansion. In general, any mid-wall hardness greater than ~325 DPH would indicate a nil-ductility temperature greater than room temperature for that particular section. Therefore, all six TREAT tubes contained portions of wall that possessed no ductility at room temperature. Tubes 16, 17, and 18 which contained locations of highest hardness also had the largest rupture openings.

The post-test brittleness of the cladding was accidentally demonstrated when rod 11 slipped from the manipulators and dropped approximately 12 in. onto a blotter-paper-covered plywood platform. The

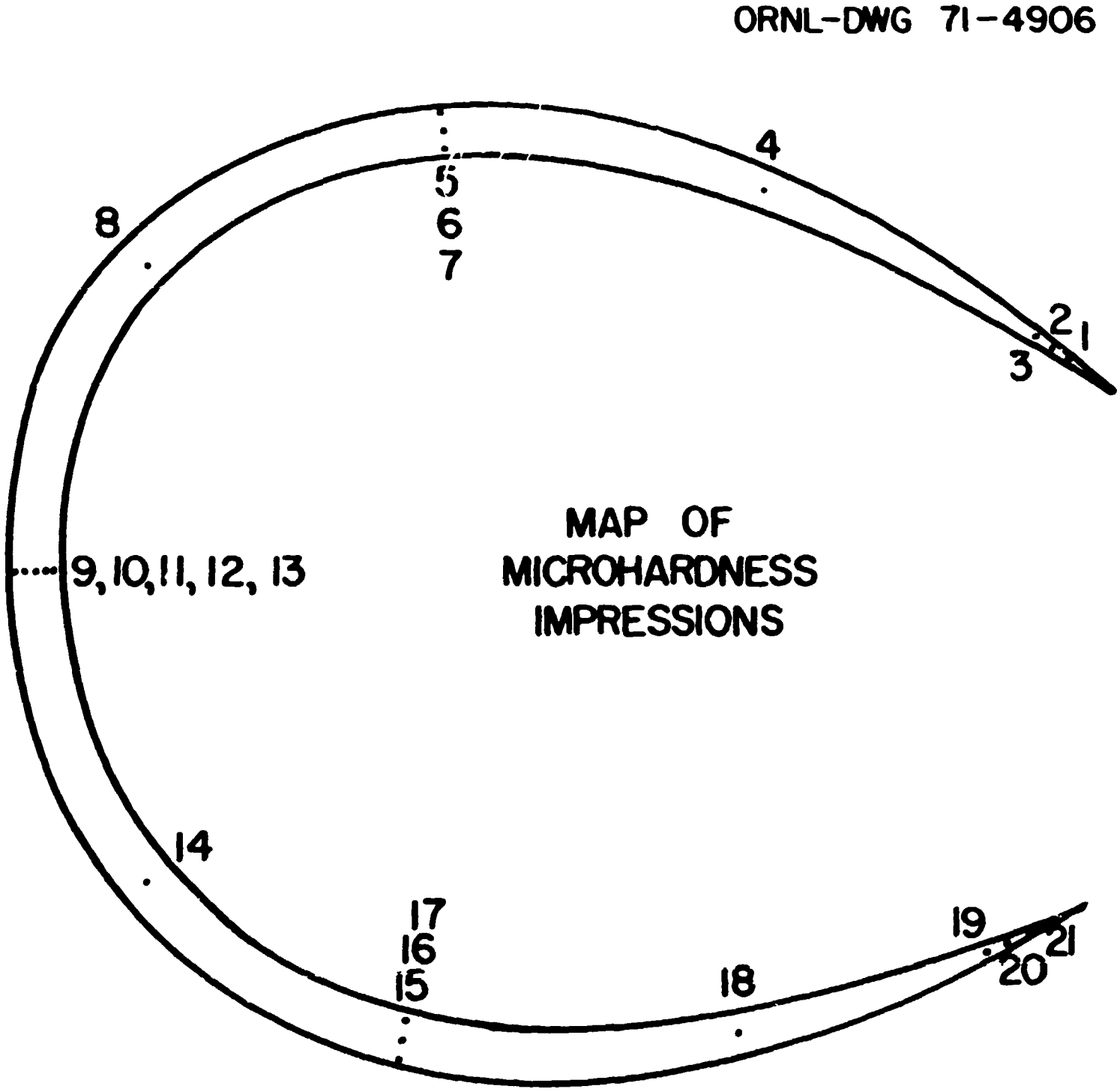


Fig. 13. Plan of Hardness Measurements Viewed from Top of Rod.

Table 4. Microhardness of Tubes from Experiment FRF-2.

| Impression Number | Tube 11 | | Tube 12 | | Tube 13 | | Tube 16 | | Tube 17 | | Tube 18 | |
|---|---|---|---|---|---|---|---|---|---|---|---|---|
| | Hardness (DPH) | Nil Ductility Temp. (°F) | Hardness (DPH) | Nil Ductility Temp. (°F) | Hardness (DPH) | Nil Ductility Temp. (°F) | Hardness (DPH) | Nil Ductility Temp. (°F) | Hardness (DPH) | Nil Ductility Temp. (°F) | Hardness (DPH) | Nil Ductility Temp. (°F) |
| 1 | 351 | 280 | 304 | < RT | 366 | 350 | 438 | 1080 | 479 | 1680 | 391 | 560 |
| 2 | 340 | 190 | 259 | < RT | 370 | 370 | 439 | 1090 | 420 | 840 | 433 | 1020 |
| 3 | 362 | 330 | 291 | < RT | 333 | 140 | 488[b] | 1840 | 386 | 500 | 470 | 1500 |
| 4 | 361[b] | < RT | 276[b] | < RT | 286[b] | < RT | 255 | < RT | 289[b] | < RT | 321[b] | < RT |
| 5 | 286 | (a) | 328 | | 295 | | 331 | | 329 | | 328 | |
| 6 | 292 | < RT | 317 | < RT | 280 | < RT | 316 | < RT | 342 | 200 | 300 | < RT |
| 7 | 365 | | 285 | | 266 | | 297 | | 308 | | 308 | |
| 8 | 275 | < RT | 290 | < RT | 268 | < RT | 319 | < RT | 308 | < RT | 253 | < RT |
| 9 | 257 | | 313 | | 279 | | 317 | | 319 | | | |
| 10 | 352 | | 295 | | 284 | | 296 | | 291 | | | |
| 11 | 275 | < RT | | | 265 | < RT | 309 | < RT | 276 | < RT | | |
| 12 | 267 | | 285 | | 249 | | 301 | | 279 | | | |
| 13 | 281 | | 302 | | 262 | | 307 | | 310 | | | |
| 14 | | | 300 | < RT | 276 | < RT | 294 | < RT | 272 | | | |
| 15 | | | 320 | | 352 | | 324 | | 336 | | | |
| 16 | | | 262[b] | < RT | 241 | < RT | 302 | < RT | 296 | < RT | | |
| 17 | Sect. Missing[c] | | 314 | | 271 | | 339 | | 317 | | | |
| 18 | | | 326 | 95 | 274 | < RT | 334 | 140 | 287 | < RT | | |
| 19 | | | 321 | 60 | 375 | 400 | 341 | 200 | 369 | 360 | | |
| 20 | | | 342 | 200 | 369 | 360 | 330 | 120 | 412 | 740 | | |
| 21 | | | 338 | 170 | 373 | 395 | 338 | 170 | 366 | 350 | | |

Footnote (c)
Section Missing

[a] Blank position indicates corresponding hardness reading taken at a position other than midwall.

[b] Local Maxima in oxide thickness.

[c] Approximate amounts missing from metallographic sections were: Rod 11, 1.0 in.; Rod 12, 0.6 in.; Rod 13, none; Rod 16, 0.4 in.; Rod 18, 1.8 in.

resulting fracture is shown in Fig. 14. Later, rod 17 and the center rod were also broken accidentally.

## Swelling Measurements

Diameters of outer rods were measured at increments along the length using micrometers in line with the ruptures and at 90°. The average diameter increases are shown in Fig. 15 for several rods. Swelling helped to provide an open path connecting the plenums with the rupture zone.

The temperatures shown in Fig. 15 were calculated from an assumed initial preheat temperature of 330°F, the increase in temperature recorded by two thermocouples, and the axial distribution of fission heat based on the measured flux profile. The flux profile was determined by gamma scans of the outer rods and is shown in Fig. 16. The solid line is an unperturbed curve expected if a TREAT fuel element occupied the experiment location. Significant flux depression occurred in the lower third of the experiment from a molybdenum liner placed there to contain melted Zircaloy cladding that might result from an accidental full-power TREAT transient.

## Coolant Channel Blockage

Individual coolant channel size could not be measured directly and would not be meaningful because of the large expansion space mentioned previously. We calculated the average circumferential strain for the seven rods at different elevations along the bundle axis and then determined the blockage created by this amount of strain confined within the square spacing of a BWR. The resulting maximum coolant channel blockage was 91% and was near the bottom of the rupture zone. Similar results from experiment FRF-1 are also shown in Fig. 17.

## Rate of Expansion of Cladding

Detailed pressure and temperature measurements are shown in Fig. 18. In order to calculate the fuel rod volume increase, we used the ideal gas law to calculate the void volume in the fuel zone, $V_3$, as a function of time:

$$nR = P\left(\frac{V_1}{T_1} + \frac{V_2}{T_2} + \frac{V_3}{T_3}\right) \quad .$$


Fig. 14. Rupture Region of Rod 11 After Fracture During Post-irradiation Examination.

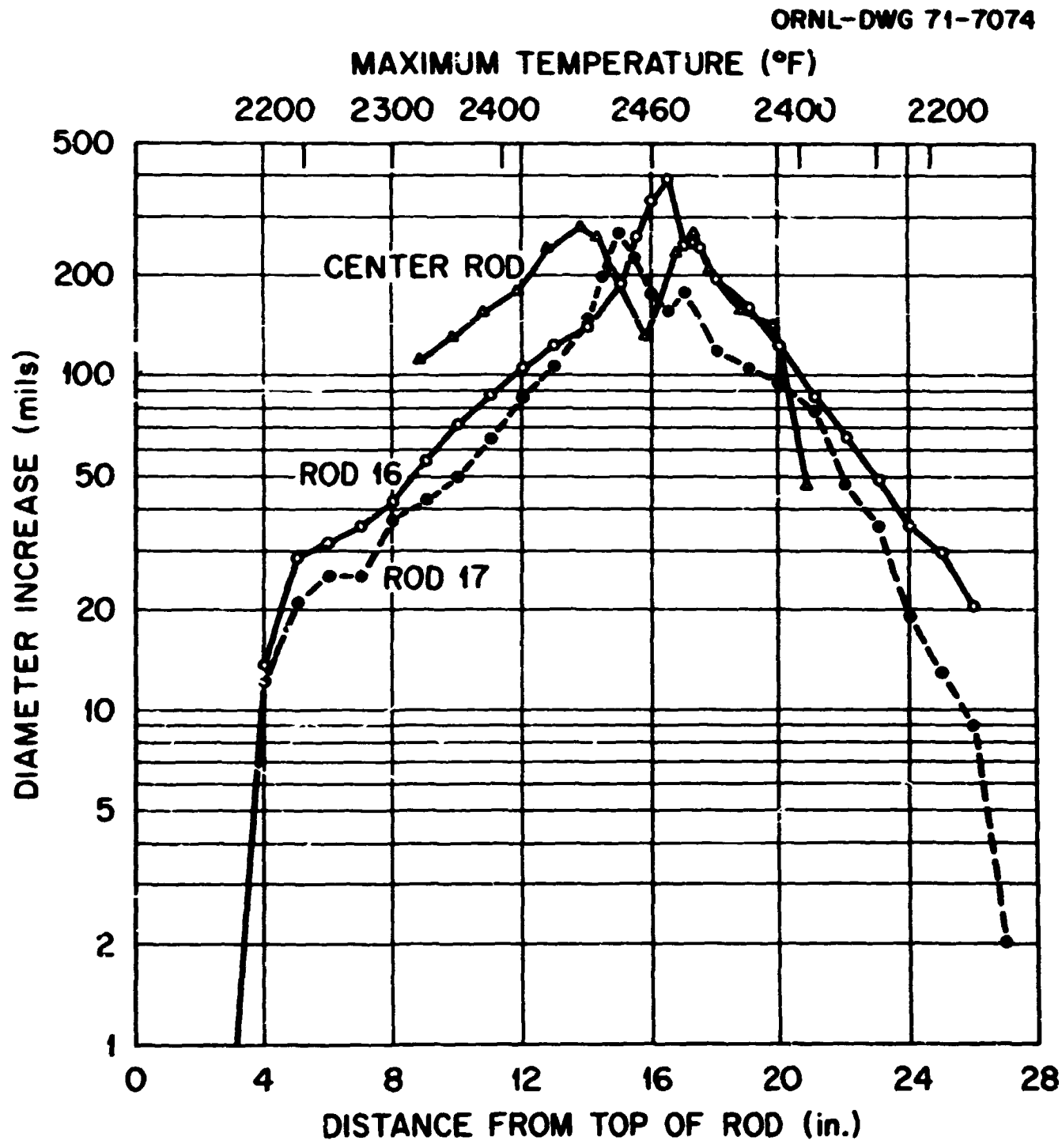


Fig. 15. Swelling of Fuel Rods in TREAT Experiment FRF-2.

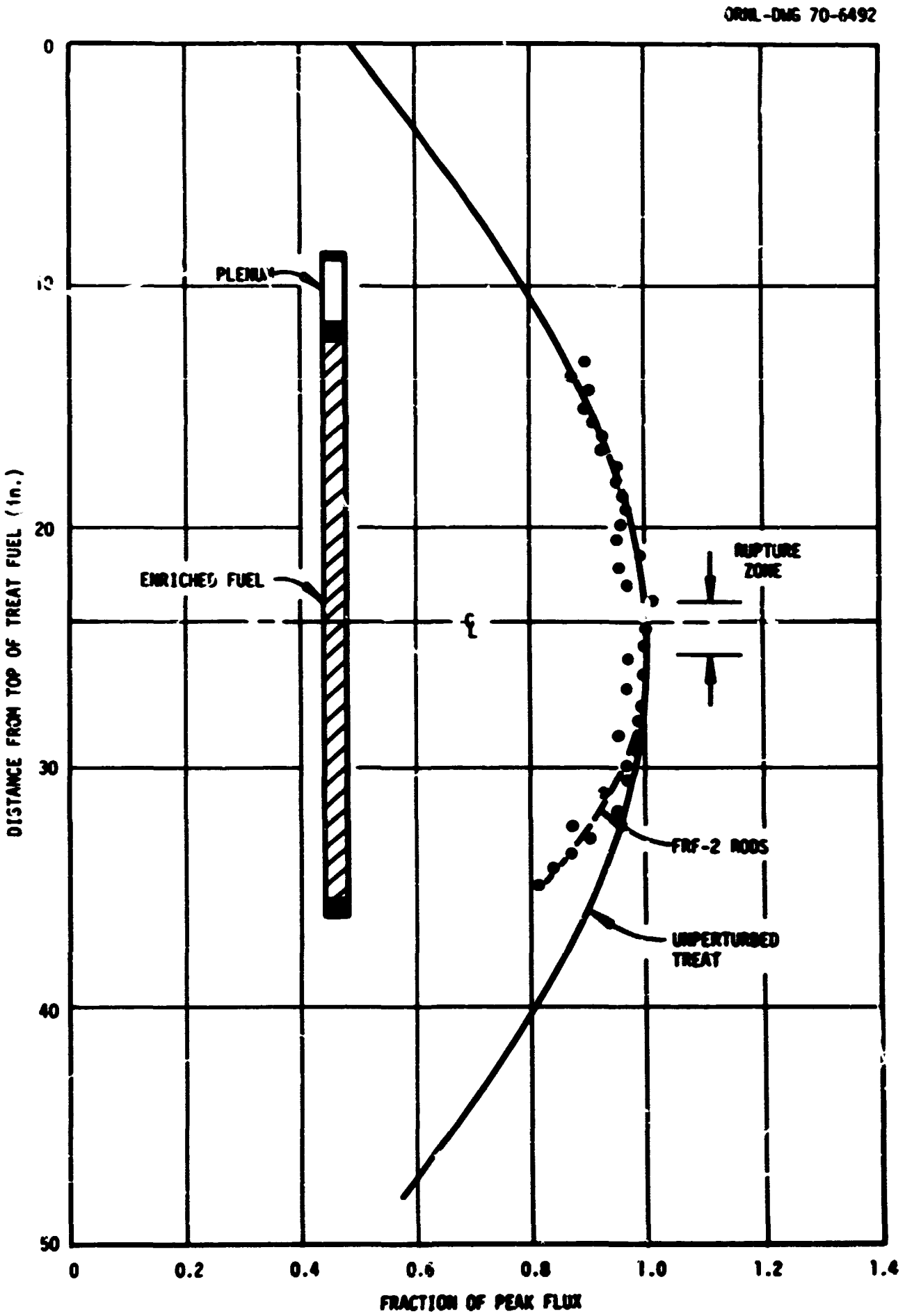


Fig. 16. Flux Profile from TREAT Irradiation of Rod 11.

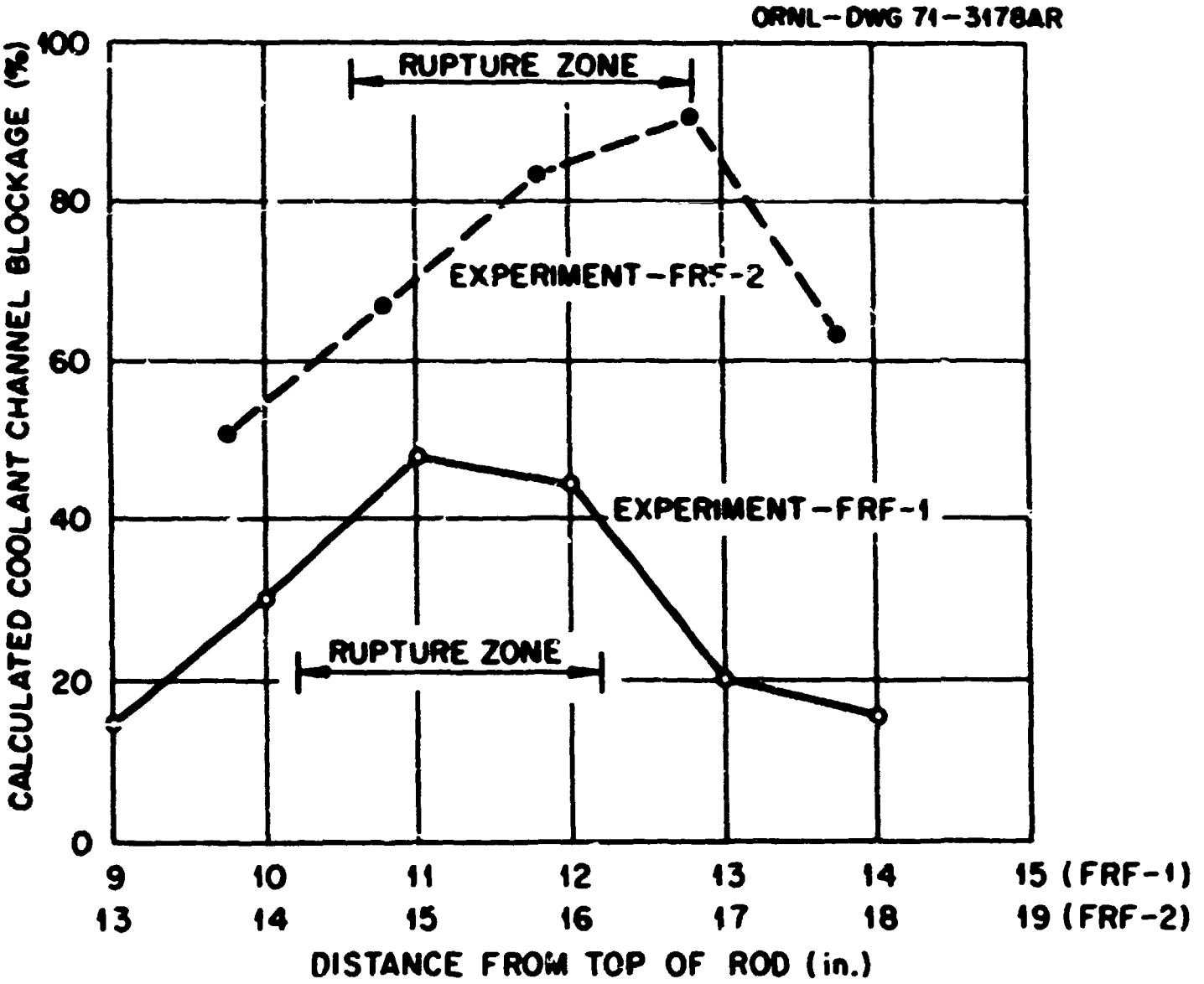


Fig. 17. Coolant Channel Blockage for BWR Rod Spacing.

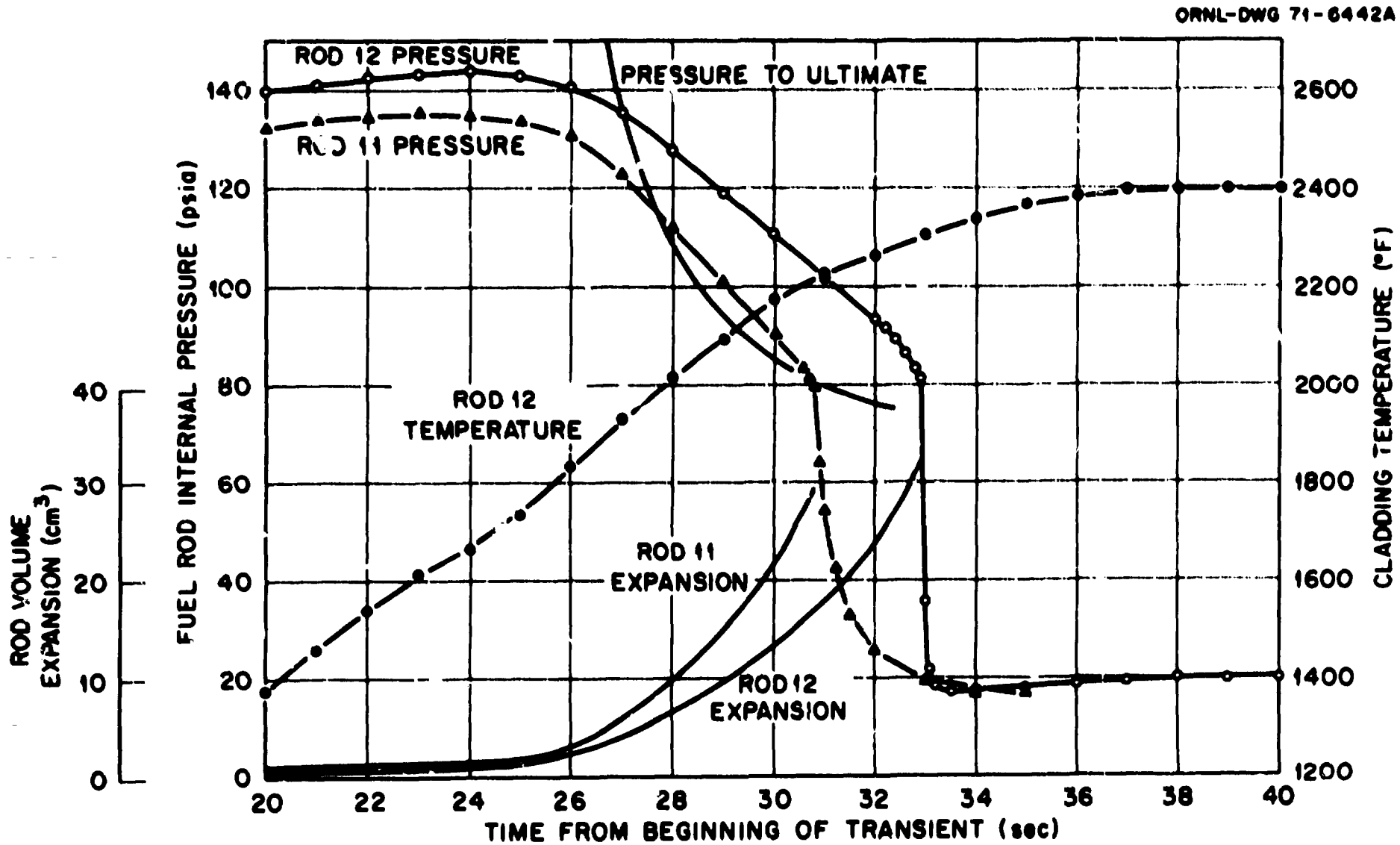


Fig. 18. Internal Pressure, Temperature, and Volume Expansion of Rods in Experiment FRF-2 in TREAT.

The product nR is constant until rupture, P is the rod pressure, $V_1$ is the pressure cell volume, $V_2$ is the volume of the fuel rod plenum, and $V_3$ is the void volume in the fuel zone of the rod. The pressure cell temperature, $T_1$, was observed to rise linearly from 255 to 270°F, whereas $T_2$, the temperature of the plenum, was estimated to increase by 60°F during the first 33 sec. The temperature of the fuel rod void volume, $T_3$, was assumed to follow the temperature recorded from thermocouple number 12-4 shown in Fig. 18. Further refinement such as providing for the fuel rod axial temperature gradient was not warranted because of limited quantity and accuracy of available data. The preheat temperature of each rod and plenum combination was calculated to agree with known initial volumes and measured initial preheat pressures. The results are shown in Fig. 18. Approximately 80% of the volume increase occurred during the 4 or 5 sec before rupture. Actual volume increases calculated from micrometer measurements for rods 11 and 12 were 29.1 and 33.4 $cm^3$, compared with calculated volumes of 29.6 and 32.6 $cm^3$, respectively.

The pressure necessary to reach the ultimate strength of the Zircaloy-4 cladding[13] is also shown in Fig. 18. The stress in the cladding was calculated by the simple hoop stress formula ($s = pr/t$) and is in general agreement with the ultimate stress.

## Fission-Product Release

The release of fission products when fuel rods rupture during a LOCA is dependent mainly on the previous time and temperature of fuel irradiation. High temperature and long irradiation time increase the diffusion of fission products from the $UO_2$ pellets into the clad gap and plenum where they are available for rapid release if the cladding ruptures during a LOCA. Long half-life fission products will accumulate in the clad gap and plenum, but the amounts of short half-life fission products in the clad gap and plenum are dependent mainly on the fuel temperature during the latest reactor operating time corresponding to one or two fission-product isotope half-lives.

Details of the center rod irradiation in the MTR and ETR were presented in the section entitled "Center Rod Irradiation." During the

LOCA simulation in TREAT, volatile and gaseous fission products were released rapidly from the clad gap and plenum of the ruptured center rod, and only small additional amounts were released from the $UO_2$. The amount released as the $UO_2$ is heated above previous operating temperature has been called the "heating burst." Both heating bursts and cooling bursts were observed when $UO_2$ pellets were heated and cooled during postirradiation annealing experiments for measurement of fission-product release.[14] Another mechanism of release during a LOCA is diffusion from the $UO_2$ pellets while the fuel remains hot.[15]

Fission-product release in TREAT experiment FRF-2 is summarized in Table 5 and complete details are given in Table 6. The fractional releases of long half-life gaseous and volatile fission products, $^{85}Kr$, $^{129}I$, and $^{137}Cs$ were similar and the release of $^{131}I$ was slightly lower.

The average release of fission products with low volatility ($^{103}Ru$, $^{89}Sr$, $^{141}Ce$, and $^{95}Zr$) to the fission-product-collection system was $1.3 \times 10^{-6}$ percent. The relative amount of uranium found in the fission-product-collection system was an order of magnitude higher.

## DISCUSSION

### Expansion Characteristics

Maximum circumferential expansion for rods in the two TREAT experiments is shown as a function of rupture temperature in Fig. 19. The reference line shown is depictive of results obtained by Hobson[16,17] with transient tube-burst tests under uniform heating conditions in inert atmosphere. An expansion minimum was found near 1700°F when Zircaloy is in the $\alpha + \beta$ two-phase region. A similar minimum was found by Busby and Marsh[18] with isothermal tube-burst tests. The comparison is good considering the differences in atmosphere, heat source, rod and plenum length, radial temperature gradient (experiment FRF-1) and irradiation of two rods.

The two center rods were irradiated in the reflector regions of the MTR and ETR so that the fast neutron fluences (>1.0 MeV) were only 1.3 and $4.6 \times 10^{19}$ nvt. According to current correlations, fast neutron effects on the physical properties of Zircaloy saturate around 2 or

Table 5. Fission Products Released in TREAT Fuel Rod Failure Experiment FRF-2

| Location | Material Found in Each Location (% of Total in Center Irrad. Rod)[a] | | | | | |
|---|---|---|---|---|---|---|
| | $^{131}I$ | $^{137}Cs$ | $^{129}Te$ | Fission Products with low Volatility[b] | U | $^{85}Kr$ |
| Primary Vessel[c] | 0.066 | 0.193 | | | | |
| Filter Pack: Deposited by diffusion | 0.042 | 0.009 | | | | |
| Filter Pack: Deposited with particles | 0.005 | 0.086 | $< 12 \times 10^{-6}$ | $1.3 \times 10^{-6}$ | $16 \times 10^{-6}$ | |
| Condensate | $<1.2 \times 10^{-6}$ | | | | | |
| Heated Charcoal | 0.0028 | | | | | |
| Total Release | 0.115 | 0.288 | | | | 0.48 |

[a]FRF-2 irradiated 62.7 full-power days to 2800 MWd/MT peak burnup at 13.9 kW/foot peak linear power, peak/average flux 1.15, total fissions $4.3 \times 10^{21}$.

[b]Median of $^{89}Sr$, $^{95}Zr$, $^{103}Ru$, and $^{141}Ce$.

[c]Primary vessel leached with 0.5 N $NH_4OH$. Only soluble materials reported.

Table 6. Fission Products Released in TREAT Fuel Rod Failure Experiment FRF-2

| Location | Material Found in Each Location (% of Total in Center Irradiated Rod) | | | | | | | | | |
|---|---|---|---|---|---|---|---|---|---|---|
| | $^{129}I$[a] | $^{131}I$ | $^{137}Cs$ | $^{129}Te$ | $^{103}Ru$ | $^{89}Sr$ | $^{141}Ce$ | $^{95}Zr$ | U[b] | $^{85}Kr$ |
| Primary Vessel[c] | 0.141 | 0.066 | 0.193 | | | | | | | |
| Housing and Flow Diffuser | 0.041 | 0.0152 | 0.0088 | $\sim 2.4\times10^{-6}$ | $0.24\times10^{-6}$ | $0.26\times10^{-6}$ | $0.12\times10^{-6}$ | $0.28\times10^{-6}$ | $9.2\times10^{-6}$ | |
| Diffu. Coil - 1 | | 0.0110 | 0.0035 | | | | | | | |
| Diffu. Coil - 2 | | 0.0063 | 0.0027 | | | | | | | |
| Diffu. Coil - 3 | | 0.0045 | 0.0024 | | | | | | | |
| Diffu. Coil - 4 | | 0.0040 | 0.0017 | | | | | | | |
| (Total of Coils) | | (0.0258) | (0.0103) | $<6\times10^{-6}$ | $<0.08\times10^{-6}$ | $\sim 0.55\times10^{-6}$ | $0.023\times10^{-6}$ | $<0.001\times10^{-6}$ | $0.36\times10^{-6}$ | |
| Filter No. 1 | | 0.0035 | 0.0760 | $<4\times10^{-6}$ | $0.76\times10^{-6}$ | $1.34\times10^{-6}$ | $1.1\times10^{-6}$ | $0.93\times10^{-6}$ | $6.0\times10^{-6}$ | |
| Filter No. 2 | | ~0.0002 | 0.00004 | | | | | | | |
| Filter No. 3 | | ~0.0002 | 0.00004 | | | | | | | |
| Backup Diffu.Coil | | 0.0016 | $5\times10^{-6}$ | | | | | | | |
| (Total Filter Pack) | | (0.047) | (0.095) | $<12\times10^{-6}$ | $<1.0\times10^{-6}$ | $\sim 2\times10^{-6}$ | $1.2\times10^{-6}$ | $1.2\times10^{-6}$ | $15.3\times10^{-6}$ | |
| Condensate, Unit-1 | | <0.00006 | | | | | | | | |
| Condensate, Unit-2 | | <0.00006 | | | | | | | | |
| Heated Charcoal, Unit-1 | | 0.00023 | | | | | | | | |
| Heated Charcoal, Unit-2 | | 0.0026 | | | | | | | | |
| Cold Charcoal | | | | | | | | | | 0.48 |
| TOTAL RELEASE FROM ROD | 0.27[d] | 0.115 | 0.288 | | | | | | | 0.48 |
| Inside Surface of Center Rod | 0.059 | | 0.034 | | | | | | | |

[a]Only the samples were analyzed for $^{129}I$.

[b]The uranium release was based on total of 5288 g $UO_2$ in 7 rods (4660 g U).

[c]The primary vessel was leached with 0.5 M $NH_4OH$ and only the soluble materials are reported.

[d]The total release of $^{129}I$ was based on the ratio of $^{129}I/^{131}I$ in other individual samples. Total $^{129}I$ inventory in the center rod was 3.28 mg.

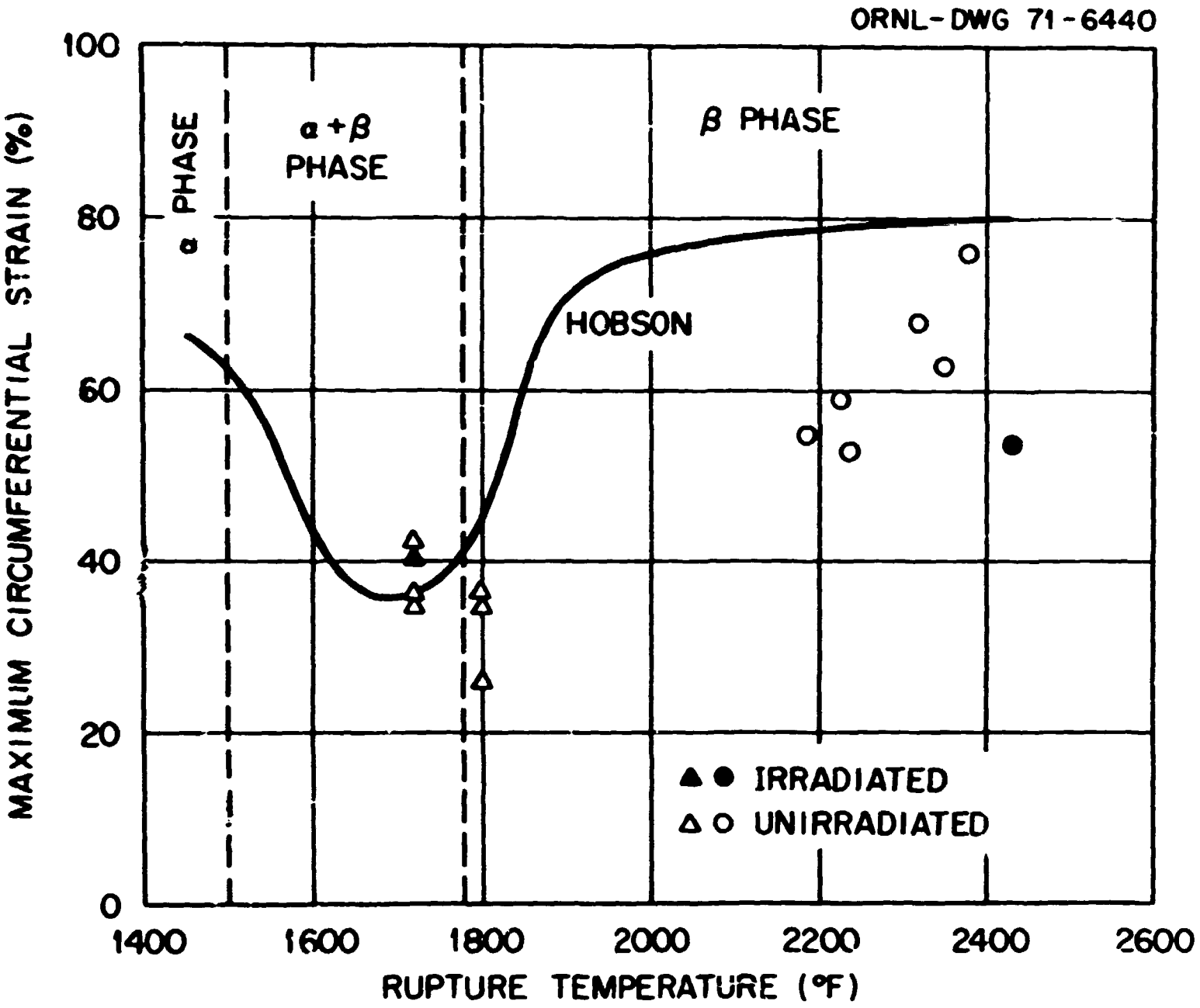


Fig. 19. Maximum Strain in TREAT LOCA Experiments.

$3 \times 10^{21}$ nvt. (Ref. 19) Using available correlations we calculated that the center rod irradiations resulted in 12 percent of saturation "damage" for FRF-1 and 22 percent for FRF-2. Juenke and White[20] used transmission electron microscopy to determine that radiation-induced damage was annealed out by a rapid temperature transient similar to those of the TREAT experiments.

Osborne[21] induction-heated fuel rods to failure in steam atmosphere using unirradiated rods and rods exposed to fast neutron fluences up to $1.4 \times 10^{21}$ nvt (7,000 MWd/MT burnup) and found the average circumferential expansion for the irradiated rods to be only 70 percent of that for the unirradiated rods. General Electric Company[22] and Westinghouse Electric Corporation[23] performed tube burst tests with pieces of irradiated tubing and also observed some reduction of expansion with irradiation.

Hobson[16,17] explored the effect of wall thickness variations on maximum expansion. Smaller expansion with wall thickness variation was qualitatively demonstrated in experiment FRF-2 with rods 16, 17, and 18 where the difference between thick and thin sides of the eccentric tubing averaged 0.0036 in. at individual cross sections. Rod 17 with the thin side toward the center (Fig. 7) swelled the least, as was expected.

The measured expansions were equivalent to BWR bundle coolant channel blockages of 48% and 91% at the worst location in the two respective experiments. Greater expansion and blockage might be expected without the large radial temperature gradients of the TREAT tests. Waddell[24,25] reported results of the tube-burst tests with 13-rod bundles of unirradiated rods and Rittenhouse[26] reported that tests with 32-rod bundles in the same series confirmed greater channel blockage toward the interior.

Expansion and rupture were not significantly affected by steam oxidation. That is, the ruptures were all ductile. The cladding was relatively brittle when examined after the experiment, but all the rods survived the normal disassembly and examination prodecure.

## Strength Characteristics

The effective stress at failure temperature for Zircaloy tubing was correlated by White[27] based on a secondary creep equation. His correlation

for inert atmosphere is shown in Fig. 20 along with effective stress calculated for one rod in each TREAT experiment at approximately two-second intervals before rupture. The TREAT cladding effective stress was calculated by the equation:

$$S_o = \frac{\sqrt{3}}{2} \frac{pr}{t}$$

where

$S_o$ = effective stress in plastic flow,
$p$ = pressure difference across the tube wall,
$r$ = initial internal radius, and
$t$ = initial wall thickness.

The factor $\sqrt{3}/2$ accounts for the biaxial stress condition during plastic flow. Agreement is rather good. The ultimate strength curve is included for comparison.

White's creep model includes effects of heat-up rate and amount of expansion (strain). We calculated effective stress at time of rupture for other portions of the same rods in order to check the validity of White's model for conditions of smaller strain. Our data indicate that moderate expansion may occur at slightly lower temperature than predicted by White. The changing pressure in our rods tends to make comparisons inaccurate.

Some deviation toward higher strength (stress) would be expected in the presence of steam at temperatures above 2000°F because of oxidation-induced strengthening. Negligible steam effect would occur with high heating rates, low temperature, or with limited steam supply. Our data do not show much oxidation-strengthening effect, probably because of the fast heating rate and limited steam supply. White[28,29] used higher steam flow relative to cladding surface area and found the deviation labeled "maximum steam effect" in Fig. 20. His isothermal tube burst tests in steam showed significantly reduced rates of expansion (strain).

## Fission-Product Release

The release of $^{129}Te$, U, and the fission products with low volatility ($^{89}Sr$, $^{95}Zr$, $^{103}Ru$, and $^{141}Ce$) was strongly affected by conditions in the second experiment. The difference from experiment FRF-1 may be seen

ORNL-DWG 71-6441

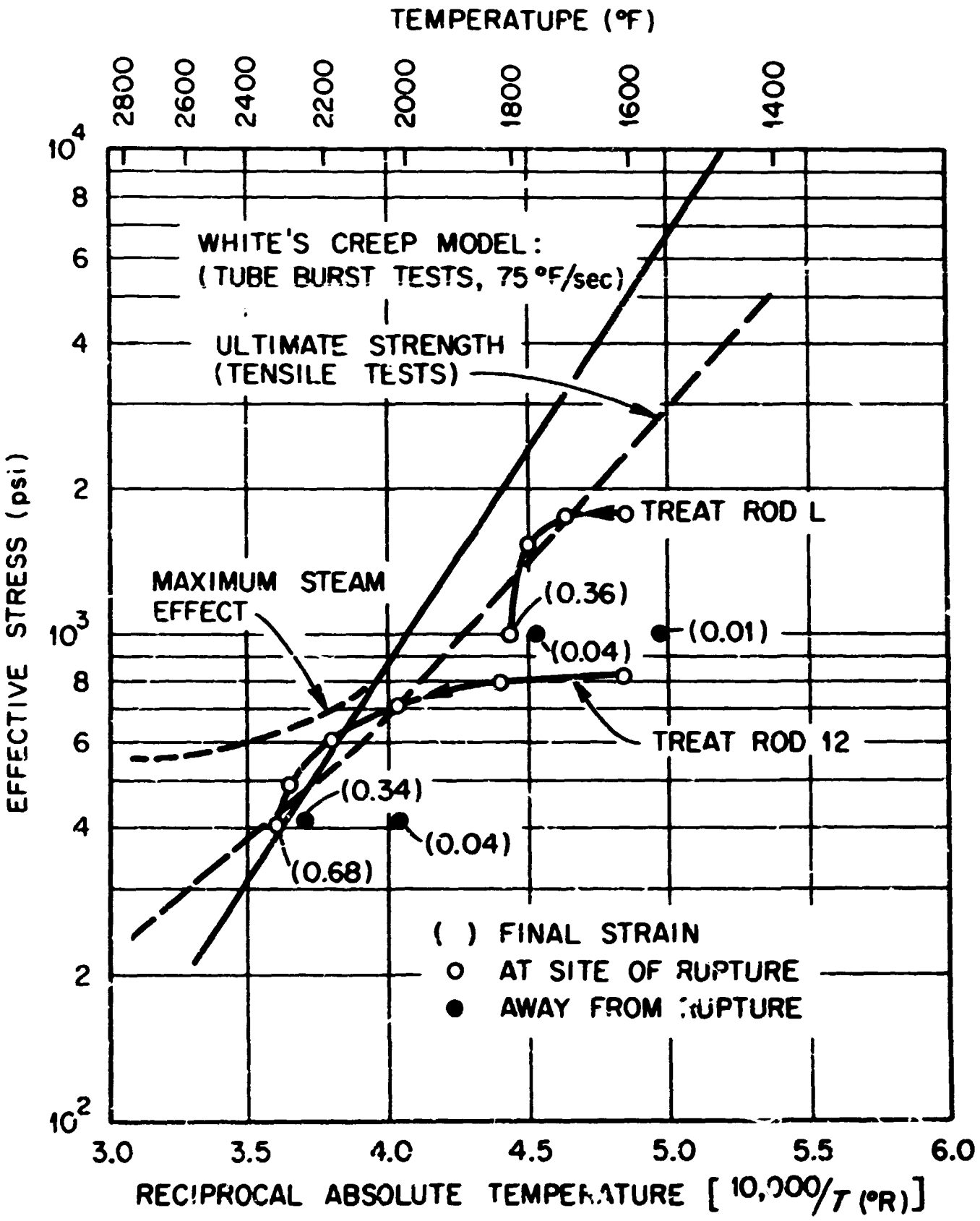


Fig. 20. Correlation of Effective Stress with Cladding Temperature.

in Table 7. The small rupture opening in the center rod restricted access of steam so that the interior of the rod remained strongly chemically reducing by action of hot zirconium. At the higher temperature of the second experiment, the external surface of the Zircaloy cladding was sufficient to react nearly quantitatively with the steam to form a hydrogen-rich atmosphere. In the LOCA temperature range, the release of fission products with low volatility is much greater in an oxidizing atmosphere.[30] The effect of a reducing atmosphere and the presence of Zircaloy cladding on tellurium behavior was demonstrated previously when Zircaloy-clad, stainless steel clad, and bare $UO_2$ fuel pins were melted in a helium atmosphere.[31] We expect that conditions in a reactor LOCA would result in a steam supply greater than that in these experiments so that the release of tellurium, uranium, and fission products with low volatility would be considerably greater than that observed in experiment FRF-2.

The release of volatile and gaseous fission products was also lower than expected. This was the result of low release from the $UO_2$ pellets into the fuel rod void spaces during the irradiation of the center rod in the ETR. The irradiation conditions were intended to be similar to those of a medium-to-high power density rod of a modern power reactor where fission-gas release would be between 1% and 10% for a short irradiation. The D′ (empirical) method was used to estimate fission-gas release from $UO_2$ into the fuel rod plenum and void spaces during the MTR and ETR irradiations.[11] This calculational method is based on fission-gas release from a series of capsule (short rod) irradiations performed by AECL (Atomic Energy of Canada Limited) and correlates fission-gas release with linear power and irradiation time, but does not include correlations for $UO_2$ temperature variances caused by cladding temperatures or clad gap conductivities different from those of the reference capsules.

The center rod peak linear power was 13.9 kw/ft, based on a radiochemical burnup analysis. The peak to average ratio was 1.15, based on an ETR flux profile so that the average rod linear power was 12.1 kw/ft. Based on previous calculations, the fission-gas release from a rod with axial power distribution will be the same as from a capsule operating uniformly at the average of the rod peak and rod average linear power

Table 7. Comparison of Fission-Product Release in Experiments FRF-1 and FRF-2

| Location | | Material Found in Each Location (% of Total in Center Rod) | | | | | |
|---|---|---|---|---|---|---|---|
| | | $^{85}Kr$ | $^{131}I$ | $^{137}Cs$ | $^{129}Te$ | Low Volatility F. P. | U |
| Primary vessel | FRF-1 | | 0.054 | 0.046 | | | |
| | FRF-2 | | 0.066 | 0.193 | | | |
| Filter Pack | FRF-1 | | 0.120 | 0.010 | 0.015 | ~900 x $10^{-6}$ | 240 x $10^{-6}$ |
| | FRF-2 | | 0.047 | 0.095 | <12 x $10^{-6}$ | ~1. x $10^{-6}$ | 16 x $10^{-6}$ |
| Heated Charcoal | FRF-1 | | 0.013 | 0 | 0 | 0 | 0 |
| | FRF-2 | | 0.0028 | 0 | 0 | 0 | 0 |
| Total Release | FRF-1 | 0.09 | 0.19 | 0.06 | | | |
| | FRF-2 | 0.48 | 0.12 | 0.29 | | | |

ratings. Therefore the center rod of FRF-2 would be comparable to a capsule operating at 13.0 kw/ft. The reference capsules contained $UO_2$ of lower density and higher thermal conductivity so that fission-gas release from the center rod would be the same as from a reference capsule operating at 0.98 (13.0) = 12.75 kw/ft = 419 w/cm linear power. The D′ (empirical) method was used to obtain the calculated fission-product release results shown in Table 8. We use an empirical diffusion parameter for iodine four times that of xenon and krypton. The empirical diffusion parameter $D_i'$ should not be confused with the conventional diffusion coefficient D′. Actual fission-gas release was much lower than predicted, and we believe that low temperature during the ETR irradiation was the cause. As mentioned before the neutron radiograph showed no central void and the gamma scan showed no migration of fission products within the rod.

Table 8. Comparison of Calculated and Measured Release from $UO_2$

| | Fission Product Isotope | | | |
|---|---|---|---|---|
| | $^{85}Kr$ | $^{129}I$ | $^{131}I$ | $^{137}Cs$ |
| Empirical Diffusion Parameter $D_i'$ ($sec^{-1}$) | $7x10^{-11}$ | $28x10^{-11}$ | $28x10^{-11}$ | $7x10^{-11}$ |
| Calculated Release from $UO_2$ (%) | 4.4 | 8.8 | 5.2 | 4.4 |
| Measured Release from $UO_2$ Pellets (%) | 0.48 | 0.32 | 0.14 | 0.32 |
| Ratio, Calculated $UO_2$ Release/Measured $UO_2$ Release | 9 | 27 | 37 | 14 |

There was no evidence of substantial retention of iodine by the cladding or $UO_2$ when iodine release was compared with fission-gas release. The inside surface of the center rod cladding was leached for 24 hr at 77°F with 1 N $NH_4OH$ + 1 N $H_2O_2$ and the amounts of $^{129}I$ and $^{137}Cs$ found in solution were reported in Table 6. Apparently the

retention of iodine and cesium on the Zircaloy cladding was low. Feuerstein investigated the system of $I_2$ in Zircaloy and reported 90% release of iodine in 10 min at 1472°F. (Ref. 32)

Approximately 2.5% of the $^{131}I$ released from the center rod (0.0028% of the center rod inventory) was collected in the warm iodine-impregnated charcoal traps. This iodine was almost certainly transported as an unreactive organic iodide, $CH_3I$. The filter pack was designed to collect chemically reactive forms of iodine ($I_2$, HI, and HCl) and particulate iodine. The very small amount of $^{131}I$ found in the condensate samples verified that none of the iodine that reached this location was in a chemically reactive form. The solubility of the iodine compound in the condensate may be illustrated by the partition coefficient (ratio of concentration in the liquid to concentration in the gas) in collection unit No. 2. Since 8.2 $cm^3$ of water was condensed from 1800 $cm^3$ of helium (per minute) at 32°F, $P = \frac{<0.00006/8.2}{0.0026/1800} < 5.1$. For $CH_3I$, we would expect a partition coefficient of about 8.5, and for $I_2$ at low concentration, approximately 10,000.

Most of the $CH_3I$ was collected in the second unit between reference times, 1.5 min and 17.5 min. We believe that the iodine was released from the rod before the 1.5 min time (approximately 55 sec after rupture) while the rods were hottest and that most of the $CH_3I$ was formed and transported to the warm impregnated charcoal during the 1.5 to 17.5 min time period. According to Barnes et al.[33], the presence of steam and radiation and the lack of air or oxygen all contribute to the formation of methyl iodide ($CH_3I$). Durant et al.[34] investigated the importance of surface reactions in the formation of methyl iodide. Parker, Creek, and Martin[35] found that methyl iodide formed after release of iodine into the stainless-steel-lined Containment Research Installation (CRI) vessel. The amount of methyl iodide ranged from 0.03 to 0.3% of the iodine inventory for steam-air atmospheres cooling from 230°F.

The release and transport behavior of short half-life gaseous and volatile fission products formed and released during the TREAT transient are shown in Table 9. The behavior patterns of some mass chains are not clear because decay during the experiment resulted in isotopes with different physical and chemical properties. In general the data are

Table 9. Distribution of Gaseous and Volatile Fission Products Formed During TREAT Transient

| | Fission Product Characteristics | | | | | | |
|---|---|---|---|---|---|---|---|
| Isotope Diffused from $UO_2$ | $^{85}Br$(3.0m)[a] | $^{88}Kr$(2.8h) | $^{91}Kr$(9.8s) | $^{135}Xe$(9.2h) | $^{135}I$(6.7h) | $^{135}I$ | $^{140}Xe$(16s) |
| Isotope Transported | $^{85m}Kr$(4.4h) | $^{88}Kr$ | $^{91}Kr$ | $^{135}Xe$ | $^{135}I$ | $^{135}I$ | $^{140}Xe$ |
| Isotope Analyzed | $^{85m}Kr$ | $^{88}Kr$ | $^{91}Sr$(9.67h) | $^{135}Xe$ | $^{135}Xe$ | $^{135}I$ | $^{140}Ba$(12.8d)[b] |
| Yield Assumed for Calculation (T.Y. = Total Yield, I.Y. = Instantaneous Yield) | 1.3 = T.Y. $^{85m}Kr$ | 3.47 = T.Y. $^{88}Kr$ | 3.84 = I.Y. $^{91}Kr$ | 0.93 = I.Y. $^{135}Xe$ | 2.85 = I.Y $^{135}I$ | 2.85 = I.Y. $^{135}I$ | 2.30 = T.Y. $^{140}Xe$ |
| - - - - Amount Each Isotope Chain Found in Each Location (Percent of Total Formed During TREAT Transient)[c] - - - - - - | | | | | | | |
| | $^{85}Br$ | $^{88}Kr$ | $^{91}Kr$ | $^{135}Xe$ | $^{135}I$ | $^{135}I$ | $^{140}Xe$ |
| Filter Pack | | | | | | | |
| Housing and Flow Diffusee | | | | | | | <0.05 |
| Diffusion Coils | | | | | | | 0.017 |
| Filter No. 1 | | | | | | | 0.0020 |
| Filter No. 2 | | | | | | | |
| Filter No. 3 | | | | | | | |
| Backup Diffusion Coil | | | | | | | 0.0013 |
| Condensate, Unit-1 | | | 0.0022 | | | N.D.[d] | 0.0018 |
| Condensate, Unit-2 | | | Trace | | | N.D. | N.D. |
| Heated Charcoal, Unit-1 | N.D. | N.D. | 0.0046 | 0.0017 | | Trace | 0.0105 |
| Heated Charcoal, Unit-2 | N.D. | N.D. | N.D. | | 0.0066[f] | 0.013[e] | N.D. |
| Cold Charcoal, Unit-1 | 0.029 | 0.033 | 0.00017 | 0.024 | | N.D. | 0.0013 |
| Cold Charcoal, Unit-2 | 0.0090 | N.D. | N.D. | ____ | 0.0021 | N.D. | N.D. |
| TOTAL FOUND | 0.038 | 0.033 | | 0.026 | | | >0.046 |

[a] Half-life shown in parentheses.

[b] The release of $^{140}Ba$ present in the $UO_2$ pellets as a result of the ETR irradiation was insignificant.

[c] $7.5 \times 10^{16}$ fissions.

[d] Not detected.

[e] Iodine found in this location was probably transported as $CH_3I$.

[f] $^{135}Xe$ found in this location was probably transported as $CH_3\ ^{135}I$.

consistent with the hypothesis that release of gases and halogens from the rod occurred quickly and that iodine then reacted to form $CH_3I$ and was transported to the warm impregnated charcoal traps. The $^{135}Xe$ was released and transported both as $^{135}Xe$ and as its precursor, $^{135}I$. We assume that the $^{135}Xe$ found in unit No. 1 was transported as $^{135}Xe$ and that the $^{135}Xe$ found in unit No. 2 was transported as $^{135}I$, so we used the respective instantaneous yields for the calculations.

## CONCLUSIONS

The two TREAT fuel rod failure experiments were conducted under the most realistic LOCA conditions of any experiment to date. Fission heating in the $UO_2$ pellets provided close duplication of the heat transfer conditions between pellets and cladding expected in a LOCA.

In both experiments we found that the ruptures and swollen areas were close together, within a 2-1/4-in. axial length. This indicates high sensitivity to temperature and lower sensitivity to random defects such as wall thickness or strength variations. The magnitude of maximum expansion and the rupture characteristics were in general agreement with tube burst tests performed in inert atmosphere in spite of experimental differences such as atmosphere, heat source, and radial temperature gradients. Measured expansion of rods in experiment FRF-2 was equivalent to blocking 91% of the bundle coolant channel area at the worst horizontal plane. Larger bundles confined to reactor-fuel-rod spacing must be ruptured under realistic accident conditions in order to determine more accurately the meshing and channel blockage characteristics that might occur in a reactor LOCA.

The fractional releases of volatile fission products $^{129}I$, $^{131}I$, and $^{137}Cs$ were only slightly lower than that of the fission gas $^{85}Kr$, an indication that credit should not be assumed for gross retention of $^{131}I$ on the surfaces of Zircaloy cladding undergoing loss-of-coolant accident conditions. Total fission-product release was low, apparently because of the irradiation conditions in the MTR and ETR. As with the first TREAT experiment, a large proportion of $^{131}I$ released from the fuel rods was in a chemically unreactive form (probably $CH_3I$) indicating that the particular combination of temperature, atmosphere, containment

material and concentration might be conducive to the formation of organic iodides.

## ACKNOWLEDGMENTS

The authors gratefully acknowledge the assistance of W. J. Martin and M. F. Osborne in performing the experiments, D. C. Hobson for the metallography, E. C. Adamson of TAN Hot Cell, and J. F. Boland and L. J. Harrison of the TREAT staff. This research was sponsored by the U.S. Atomic Energy Commission under contract with Union Carbide Corporation.

## REFERENCES


1. C. G. Lawson, Emergency Core Cooling Systems for Light-Water Power Reactors, USAEC Report ORNL-NSIC-24 (September 1968).

2. P. L. Rittenhouse, Failure Modes of Zircaloy-Clad Fuel Rods, USAEC Report ORNL-TM-2374, Oak Ridge National Laboratory (September 1968).

3. P. L. Rittenhouse, Failure Modes of Zircaloy-Clad Fuel Rods, Part 2: Program Revisions, USAEC Report ORNL-TM-2548, Oak Ridge National Laboratory (May 1969).

4. P. L. Rittenhouse, Failure Modes of Zircaloy-Clad Fuel Rods, Part 3: Description of ORNL Program, USAEC Report ORNL-TM-2742, Oak Ridge National Laboratory (January 1970).

5. P. L. Rittenhouse, Progress in Zircaloy Cladding Failure Modes Research, USAEC Report ORNL-TM-3188, Oak Ridge National Laboratory (October 1970).

6. P. L. Rittenhouse, Fuel Rod Failure and Its Effects in Light-Water Reactor Accidents, Nuclear Safety, 12(5) (Sept-Oct 1971).

7. R. A. Lorenz, D. O. Hobson, and G. W. Parker, Final Report on the First Fuel Rod Failure Transient Test of a Zircaloy-Clad Fuel Rod Cluster in TREAT, ORNL-4635, Oak Ridge National Laboratory (Feb 1971).

8. Reactor Development Program Progress Report, May 1967, pp. 122-123, USAEC Report ANL-7342, Argonne National Laboratory (1967).

9. G. W. Parker and R. A. Lorenz, "Rupture Tests of Irradiated Fuel Capsules," Nuclear Safety Program Ann. Progr. Rept. Dec. 31, 1968, USAEC Report ORNL-4374, Oak Ridge National Laboratory, pp. 84-88, (June 1969).

10. Howard A. McLain, Potential Metal-Water Reactions in Light-Water-Cooled Reactors, ORNL-NSIC-23, Oak Ridge National Laboratory (August 1968).

11. D. O. Hobson, "Evaluation of Fuel Rod Embrittlement During a LOCA," ORNL Nuclear Safety Research and Development Program Bimonthly Report for January-February 1971, USAEC Report ORNL-TM-3342, Oak Ridge National Laboratory, pp. 7-12 (May 1971).

12. D. O. Hobson, "Metallurgical Evaluation of Embrittled Zircaloy Tubing," Nucl. Safety Prog. Ann. Progr. Rept. for Period Ending Dec. 31, 1970, USAEC Report ORNL-4647, pp. 23-27 (May 1971).

13. H. C. Brassfield et al., Recommended Property and Reaction Kinetics Data for Use in Evaluating a Light-Water-Cooled Reactor Loss-of-Coolant Incident Involving Zircaloy-4 or 304-SS-Clad $UO_2$, USAEC Report GEMP-483, pp. 32-36, General Electric Company (April 1968).

14. G. W. Parker et al., Out-of-Pile Studies of Fission-Product Release from Overheated Reactor Fuels at ORNL, 1955-1965, USAEC Report ORNL-3981, pp. 75-83, Oak Ridge National Laboratory (July 1967).

15. W. A. Carbiener and R. L. Ritzman, An Evaluation of the Applicability of Existing Data to the Analytical Description of a Nuclear-Reactor Accident, Quarterly Progress Report for January through March, 1970, USAEC Report BMI-1881, pp. 12-15, Battelle Memorial Institute (April 1970).

16. D. O. Hobson, M. F. Osborne, and G. W. Parker, Comparison of Rupture Data from Irradiated Fuel Rods and Unirradiated Cladding, Nucl. Tech., 14(8) (Aug 1971).

17. D. O. Hobson and P. L. Rittenhouse, Deformation and Rupture Behavior of Light-Water Reactor Fuel Cladding, USAEC Report ORNL-4727, Oak Ridge National Laboratory (October 1971).

18. C. C. Busby and K. B. Marsh, High Temperature Deformation and Burst Characteristics of Recrystallized Zircaloy-4 Tubing, WAPD-TM-900, Bettis Atomic Power Laboratory (January 1970).

19. C. R. Woods, ed., Properties of Zircaloy-4 Tubing, WAPD-TM-585, Bettis Atomic Power Laboratory (December 1966).

20. E. F. Juenke and J. F. White, Physical-Chemical Studies of Clad $UO_2$ Under Reactor Accident Conditions, GEMP-731, pp. 18-21, General Electric Company (April 1970).

21. M. F. Osborne and G. W. Parker, The Effect of Irradiation on the Failure of Zircaloy-Clad Fuel Rods, USAEC Report ORNL-TM-3626, Oak Ridge National Laboratory (December 1971).

22. E. F. Juenke and J. F. White, Physical-Chemical Studies of Clad $UO_2$ Under Reactor Accident Conditions, GEMP-731, pp. 12-17, General Electric Company (April 1970).

23. Performance of Zircaloy Clad Fuel Rods During a Simulated Loss-of-Coolant Accident - Single Rod Tests, Vol. II, USAEC Report WCAP-7379, Westinghouse Electric Corp. (1969).

24. R. D. Waddell, Multirod Transinet Tube-Burst Tests, pp. 9-14, Nucl. Safety Prog. Ann. Progr. Rept. for Period Ending Dec. 31, 1970, USAEC Report ORNL-4647, Oak Ridge National Laboratory (May 1971).

25. R. D. Waddell, Measurement of Light-Water Reactor Coolant Channel Reduction Arising from Cladding Deformation During a Loss-of-Coolant Accident, Nucl. Tech., 14(8) (Aug 1971).

26. P. L. Rittenhouse, Analysis of Factors Affecting Fuel Rod Swelling and Coolant Channel Blockage, pp. 2-14, ORNL Nucl. Safety Res. and Dev. Prog. Bimon. Report for Nov-Dec 1970, USAEC Report ORNL-TM-3263, Oak Ridge National Laboratory (March 1971).

27. E. F. Juenke and J. F. White, Physical-Chemical Studies of Clad $UO_2$ Under Reactor Accident Conditions, USAEC Report GEMP-731, pp 2-10, General Electric Company (April 1970).

28. ibid, pp 1-4.

29. J. F. White, Physical-Chemical Studies of Clad $UO_2$ Under Reactor Accident Conditions, pp. 203-209, Eighth Annual Report - AEC Fuels and Materials Development Program, USAEC Report GEMP-1012, Part II, General Electric Company (March 1969),

30. G. W. Parker et al., Out-of-Pile Studies of Fission-Product Release from Overheated Reactor Fuels at ORNL, 1955-1956, USAEC Report ORNL-3981, pp. 75-93, Oak Ridge National Laboratory (July 1967).

31. ibid, pp. 99, 100.

32. Horst Feuerstein, Behavior of Iodine in Zircaloy Capsules, USAEC Report ORNL-4543, pp. 19-25, Oak Ridge National Laboratory (Aug 1970).

33. Russell H. Barnes, James L. McFarling, John F. Kircher, and Charles W. Townley, Studies of Methyl Iodide Formation Under Nuclear-Reactor-Accident Conditions, BMI-1829, Battelle Memorial Institute (Feb 1968).

34. W. S. Curant, R. C. Milham, D. R. Muhlbaier, and A. H. Peters, Activity Confinement System of the Savannah River Plant Reactors, USAEC Report DP-1071, Savannah River Laboratory (August 1966).

35. G. W. Parker, G. E. Creek, and W. J. Martin, Fission Product Transport Behavior in the Stainless Steel Lined Containment Research Installation (CRI), USAEC Report ORNL-4502, pp. 86-94, Oak Ridge National Laboratory (February 1971).